Response to Referee #1

We thank the reviewer for the useful suggestions to improve the paper. The comments of the referee are repeated in bold letters while our response is given in normal text.

According to the comments of both referees, we changed to title of the paper, replaced X by [X], and added error bars to the TIMED/SABER observations in Fig. 1-5.
We further carried out sensitivity runs with different sets of Einstein coefficients and included a new Figure 2. We also increased the uncertainty of the Einstein coefficients and added uncertainties of SABER temperature, SABER OH(9-7)+OH(8-6) VER, and SABER O3, resulting in larger total uncertainties of [O(3P)] and [H]. The discussion of potential error sources of [O(3P)] was also extended.
The rate of OH(v=8)+O(3P) was reduced in order to obtain physically allowed [O(3P)] values, which are slightly lower than in the previous paper version.
Finally, a detailed comparison between the [O(3P)] derived here and [O(3P)] from other studies is also included in the section "Conclusions" and we explicitly state that out [O(3P)] should be regarded as an upper limit.

General comments:

I know it's a bit persnickety, but throughout the paper you need to be careful distinguishing between X and [X], as is done in the equations. X is not being derived, you are deriving X densities, or deriving [X].
Done, we changed X to [X] throughout the paper.

If O3 is also a variable in the airglow model, could you not compare the resulting O3 with SABER values as a further constraint, in addition to the SABER VER? Either way, it would be interesting to see how the best fit model O3 compares to the SABER values, since those are not related to OH (although if it is expected that SABER O3 values are too large, maybe this wouldn't work. Or could you compare to SABER O3 1.27 µm data?).
No, O3 is not a variable in this paper and was obtained from SABER observations at 9.6 µm. Comparisons with SABER O3 at 1.27 µm are not possible since these measurements are not available during night. Recent comparisons between SABER night-time O3 with MIPAS night-time O3 showed that these two data sets agree within the corresponding error bars in the altitude region 80-100 km over the equator region (Lopez-Puertas et al., 2018, their Fig. 8 and 10). Thus, at least to our knowledge there is no conclusive evidence stating that SABER night-time O3 is generally too large or too low. The corresponding sentences in the paper were rephrased and an uncertainty of about 10 % of SABER O3 (Smith et al., 2013) was considered when estimating the total error of derived [O(3P)] and [H] profiles.

Thus, we added (l. 166-167):
"There are also SABER O_3 measurements at 1.27 µm but these observations are not available during night."

rewrote l. 211-216:
“Finally, rewriting Eq. (1) enables the derivation of [H] while [O(^{3}P)] is calculated by substituting Eq. (3) in Eq. (1) and rewriting the resulting term as follows:

$$[\mathrm{H}] = \frac{\mathrm{OH}(9-7) + \mathrm{OH}(8-6)\ \mathrm{VER}}{\mathrm{G}\, k_1 [\mathrm{O_3}]} \quad , \tag{4a}$$

$$[\mathrm{O}(^3\mathrm{P})] = \frac{\mathrm{OH}(9-7) + \mathrm{OH}(8-6)\ \mathrm{VER}}{\mathrm{G}\,(k_3 [\mathrm{O_2}][\mathrm{M}] - k_2 [\mathrm{O_3}])} . \tag{4b}$$

Air temperature and air pressure from SABER were used to calculate [M], [O_2] (VMR of 0.21), and [N_2] (VMR of 0.78) as well as to convert SABER O_3 VMR into [O_3] via the ideal gas law.”

and added l. 549-554:
“Recent comparisons between MIPAS O_3 and SABER O_3 derived at 9.6 µm were performed by Lopez-Puertas et al. (2018). The authors showed that night-time O_3 from SABER is slightly larger than night-time O_3 obtained from MIPAS in the altitude region 80-100 km over the equator (their Fig. 8 and 10) but these differences are within the corresponding errors. Thus, at least to our knowledge there is no conclusive evidence stating that SABER night-time O_3 is generally too large. Nevertheless, we considered an uncertainty of O_3 of about 10 % (Smith et al., 2013).”

Also, please comment on how initial conditions of the target species affect the results of the model, i.e. have you tested this, what are the scale of any uncertainties the first guesses can add?
The target species [O(3P)] and [H] were derived by Eq. 4a and 4b, solely depending on OH airglow, [O3], [O2], [M], and several rates of chemical and physical processes involved (k1, k2, k3, G).

$$[\mathrm{H}] = \frac{\mathrm{OH}(9-7) + \mathrm{OH}(8-6)\ \mathrm{VER}}{\mathrm{G}\, k_1 [\mathrm{O_3}]} \quad , \tag{4a}$$

$$[\mathrm{O}(^3\mathrm{P})] = \frac{\mathrm{OH}(9-7) + \mathrm{OH}(8-6)\ \mathrm{VER}}{\mathrm{G}\,(k_3 [\mathrm{O_2}][\mathrm{M}] - k_2 [\mathrm{O_3}])} . \tag{4b}$$

During our sensitivity runs, we used different [O(3P)] and [H] values based on different assumptions of the chemical and physical rates involved.
But we did not assume any a priori information of [O(3P)] and [H] to calculate these two target species, and consequently there are no “initial conditions” of the target species [O(3P)] and [H] influencing the model results.

Thus, we rephrased (l. 220-222):
“It is apparent from Eq. (4a-b) that any changes applied to the input parameters (G, O_2, O_3, M, k_1, k_2, k_3) are balanced by the derived values of [O(^{3}P)] and [H], without assuming any a priori information of [O(^{3}P) and [H].”

Specific comments:

Abstract should specifically indicate that the [O] and [H] profiles derived in this study are from the SABER observations using an OH model informed by SCIAMACHY and SABER observations.
We rewrote the beginning of the Abstract as follows (l. 10-16):
"Based on the zero dimensional box model CAABA/MECCA-3.72f, an OH airglow model was developed to derive night-time number densities of atomic oxygen ([O(^{3}P)]) and atomic hydrogen ([H]) in the mesopause region (~75-100 km). The profiles of [O(^{3}P)] and [H] were calculated from TIMED/SABER satellite OH airglow emissions measured at 2.0 µm. The two target species were used to initialize the OH airglow model, which was empirically adjusted to fit four different OH airglow emissions observed by the satellite/instrument configuration TIMED/SABER at 2.0 µm and at 1.6 µm as well as measurements by ENVISAT/SCIAMACHY of the transitions OH(6-2) and OH(3-1)."

L27: "high" should be "large" (as to not confuse with altitude)
Sentence was rephrased.

L39 and onward: What is meant by "OH(v)"? Do you mean vibrationally excited OH? It should be defined when it is first used as "vibrationally excited OH" or "OH(v>0)".
We rephrased l. 38-39 and adapted the text onward:
"This chemical reaction additionally leads to the production of vibrationally excited hydroxyl radicals (OH(v>0)) up to the vibrational level v=9, …"

L63: "last decades" sounds ominous. Should be specific, i.e. last three to four decades.
Done. Was changed as suggested by the referee.

L69: "of" should be "from"
Done.

L79: "individually" doesn't sound right. Maybe, "Both airglow emissions were used to derive separate data sets of O(3P) profiles"?
and
L80: "profiles" makes it sound as if only one profile was retrieved for each airglow feature. Should probably be "data sets".
Done. Sentence was changed to:
"Both airglow emissions were used to derive separate data sets of [O(^{3}P)] and the best agreement between these two [O(^{3}P)] data sets was obtained …"

L89: should be OH(v=9). Or define that OH(x) means OH(v=x).
Done, the notation of OH(x) was changed to OH(v=x) throughout the paper.

L140: please fix the significant digit mismatch for "837.5-848"
Done, was changed to: "837.5-848.0".

L183: by "issues" do you mean uncertainties?
We changed "issues" to "uncertainties".

L205-208: should specify that the three-body reaction is the production of O3.
Was changed to:
"In the second step, chemical equilibrium of O_3 during night is assumed as follows:

$$k_1[H][O_3] + k_2[O(^3P)][O_3] = k_3[O(^3P)][O_2][M], \quad (3)$$

meaning that O_3 loss due to H and $O(^3P)$ (left side) is balanced by O_3 formation via the three-body-reaction $O(^3P)+O_2+M$ (right side)."

L209: M is not the total density of air, M represents an air molecule. [M] is the total density.
Was changed to:
"while *M* being an air molecule and [M] being the total number density of the air."

L215-216: The wording makes it sound as if the SABER O3 was derived via the ideal gas law. Did you mean to say that you're using SABER derived O3?
Yes, we meant that the O3 volume mixing ratios from SABER were converted into O3 number densities.

Thus, we rephrased this sentence to:
"Air temperature and air pressure from SABER were used to calculate [M], $[O_2]$ (VMR of 0.21), and $[N_2]$ (VMR of 0.78) as well as to convert SABER O_3 VMR into $[O_3]$ via the ideal gas law."

L234-235: would suggest "well suited" as opposed to "very suited".
Done.

L248-250: the way this sentence is worded means that the equation should be v=9. If that's not the case, it should read something like "OH at all vibrational levels v≤9"
The sentence was rephrased to:
"The reaction $H+O_3$ can populate OH(v) at all vibrational level $v \leq 9$ and the nascent distribution of OH(v) was taken from Adler-Golden (1997)."

L264: I assume that by "added" you mean "applied" and not literally added.
Yes, you assumed right. Since a factor cannot be added, we replaced "added" with to "applied".

Figures 1-5: Why are there no error bars on the SABER observations?
We added error bars of OH(5-3)+OH(4-2) VER in Fig.1-5 and a short description
as follows (l. 176-181):

"The total uncertainty of SABER OH airglow data used here comprises three different error sources. Since we used climatology of the measurements (see Sect. 2.2), there are sufficient samples that the random noise component of the total uncertainty is essentially zero. The remaining two major terms are the absolute calibration error (<5 %) and the "unfilter" factor error (<3 %). Assuming a root-sum-square propagation of the individual uncertainties, this results in a total uncertainty of about 6 % for all data points presented in this study."

L396: "probably" is not needed
Was deleted.

L402: They also seem to match within the error bars above ~92 km.
and
L402-404: I believe this sentence is missing an altitude value and a very important comma. Are you intending to say, "The model still overestimates the measurements in the altitude region above xx km, which might be related to O(3P) quenching."?
This section was rephrased as follows (l. 400-404):
"This new model is referred to as "O_2 SD model" and the corresponding results are displayed in Fig. 3 as red lines, showing that the simulated OH(6-2) VER matches the observations within the error bars below 85 km and above ~92 km. The model still overestimates the measurements in the altitude region ~90 km, which might be related to O(^{3}P) quenching (see Sect. 3.3)."

R8: this claims that you're only considering $0 \leq v' \leq v-5$, for $v \geq 6$. If that were the case, then the branching ratios for 8-4, and 7-3 should be 0, which, according to Table 2, they are not. Should it be $0 \leq v' \leq v-4$?
This is a typing error. It has to be "$v' \leq 5$" and not "$v' \leq v-5$".
Thus, we corrected R8 to: $OH(v \geq 6)+O_2 \rightarrow OH(v' \leq 5)+O_2$

L432: "Including R10b in the model…" is confusing.
In the v-4 scenario, are you including R10a and R10b, or are you including only R10b and not R10a. If it's the former, that would seem to imply that v'=v-4 can't occur at all (for $v \geq 6$), and then, again, the branching ratios for 8-4, and 7-3 should be 0. If it's the latter, then I agree that the implication is that v'=v-5 (and not v'=v-4) is the predominant pathway, which fits with the values in Table 2. Please make the explanation of this case clearer. (It's even more confusing in the context of R8, which already says this pathway isn't being considered.)
We meant the latter case, in which R10a is substituted by R10b.
Thus, we rephrased the sentence to: "Replacing R10a by R10b in the model…"

L460: Should be "that implied" instead of "which implied".
Also, "implied" is somewhat vague and makes it sound like you might not be sure (same with "seems reasonable").
Done. We changed "which implied" to "that showed" and "seems reasonable" to "is reasonable".

Table 3: Reactions 11a-d seem to indicate that k11 doesn't entirely decrease with v, which goes against what's written in the text. This is touched on a bit later, but not explicitly stated.
The rate of $OH(\nu=8)+O(^3P)$ was reduced and the corresponding explanation in the text was extended as follows (l. 473-486):
"The assumption that $k_{11}(\nu)$ decreases at lower vibrational levels is supported by the overall rate of $OH(\nu=7)+O(^3P)\rightarrow OH(\nu')+O(^1D)$ at mesopause temperature which is suggested to be on the order of $0.9\text{-}1.6\times10^{-10}$ cm^3 s^{-1} (Thiebaud et al., 2010; Varandas, 2004). At least to our knowledge, the total rate of $OH(\nu=8)+O(^3P)\rightarrow OH(\nu')+O(^1D)$ was not measured. Nevertheless, results reported by Mlynczak et al. (2018) and Panka et al. (2017, 2018) indicate that this rate might be slower than the value of 2.3×10^{-10} cm^3 s^{-1} suggested by Sharma et al. (2015). This is also in agreement with our findings here, because applying 2.3×10^{-10} cm^3 s^{-1} for $k_{11}(\nu=9,8)$ results in non-physical $[O(^3P)]$ values above 90 km. The corresponding value of $[O(^3P)]$ e.g. at 95 km is about 1.25 times larger than SABER $[O(^3P)]$ 2013 (Mlynczak et al., 2013a) which in turn is about 1.15 times larger than the upper limit of $[O(^3P)]$ (Mlynczak et al., 2013b, their Fig. 4). This results in a factor of $1.15\times1.25=1.44$ (=44 %) above the upper limit and cannot be explained by the uncertainty of the $[O(^3P)]$ profile derived here (40 %, see Sect. 3.4). In order to obtain reasonable $[O(^3P)]$ values, it was necessary to lower the rate of $k_{11}(\nu=8)$ to 1.8×10^{-10} cm^3 s^{-1}, and we therefore recommend $k_{11}(\nu=8)\leq1.8\times10^{-10}$ cm^3 s^{-1} as an upper limit to derive physically allowed $[O(^3P)]$ values."

L528: "higher" should be "larger" as not to be confused with the discussion of altitude.
Done.

Figure 6: These plots would be much easier to read with boxed axes (ticks on the top and right).
Done.

Also, this would be a good spot to compare O3 and show that the model O3 is (presumably) lesser than SABER values.
As explained above, O3 was not a variable in this study. The [O3] used here was calculated from SABER O3 VMR.

L632-635: Have you considered doing a similar study incorporating OH(9-4), (8-3), and (5-1) band VERs from OSIRIS?
Not yet because our project is focused on SCIAMACHY observations. Comparisons between SCIAMACHY and OSIRIS might be hard since both instruments are on board of two different sun-synchronous satellites. The Odin satellite crosses the equator at 18 LT while ENVISAT crosses the equator at 22 LT. Thus, there might be a few co-location measurements but only at high latitudes. But replacing SCIAMACHY data by OSIRIS data should be possible and it would be very useful to compare the corresponding results to the results of this study.

Thus, we added in the text:
"Including additional OH transitions, like OH(9-4), OH(8-3), and OH(5-1) from the Optical Spectrograph and InfraRed Imager System (OSIRIS) on board the Odin satellite, might result in other values and deactivation schemes. This could be a subject of a future study."

Summary: needs a bit more description at the end of how [O] and [H] compare to the SABER results and explaining the differences.

We added (l.653-663):

"The [H] derived here is systematically larger by a factor of 1.5 than SABER [H] reported in Mlynczak et al. (2018) which is primarily attributed to their slower $OH(\nu=8)+O_2$ rate. Our $[O(^3P)]$ values in the altitude region below ~87 km are in agreement within the corresponding errors with the results found in Mlynczak et al. (2018) and Zhu and Kaufmann (2018) but are lower than the values presented in Panka et al. (2018). However, we think that the results of the latter study are too large because the authors falsely assumed too fast $OH(\nu)+O_2$ rates. In the altitude region above ~87 km, the $[O(^3P)]$ shown here is generally larger than the values reported in these three studies up to a factor 1.5 to 1.7. These differences are attributed to the faster rates and different deactivation channels of $OH(\nu)+O(^3P)$. Therefore, it is indicated that we might overestimate $[O(^3P)]$ above >87km and we suggest that our results should be interpreted as an upper limit. However, a final conclusion cannot be drawn at this point due the large uncertainties of the rates assumed to derive $[O(^3P)]$."

Response to Referee #2

We thank the reviewer for the useful suggestions to improve the paper. The comments of the referee are repeated in bold letters while our response is given in normal text.

According to the comments of both referees, we changed to title of the paper, replaced X by [X], and added error bars to the TIMED/SABER observations in Fig. 1-5.
We further carried out sensitivity runs with different sets of Einstein coefficients and included a new Figure 2. We also increased the uncertainty of the Einstein coefficients and added uncertainties of SABER temperature, SABER OH(9-7)+OH(8-6) VER, and SABER O3, resulting in larger total uncertainties of [O(3P)] and [H]. The discussion of potential error sources of [O(3P)] was also extended.
The rate of OH(v=8)+O(3P) was reduced in order to obtain physically allowed [O(3P)] values, which are slightly lower than in the previous paper version.
Finally, a detailed comparison between the [O(3P)] derived here and [O(3P)] from other studies is also included in the section "Conclusions" and we explicitly state that out [O(3P)] should be regarded as an upper limit.

General comments:

This study proposes a new OH airglow model to retrieve O and H densities in the mesosphere. The OH model is empirically developed to simultaneously fit four OH emissions observed by the SABER/TIMED instrument at 2.0- and 1.6-microns as well as the OH(6-2) and OH(3-1) bands measured by SCIAMACHY/ENVISAT. The authors show that using adjusted rate coefficients and specific state-to-state relaxation mechanisms, the OH model reproduces the four emissions. However, they retrieve very high O and H concentrations.
The concept of fitting four emission bands simultaneously is promising as it may constrain unknown parameters involved in modeling OH emissions. The conclusions regarding their new OH model, however, are speculative as model inputs used in the study to simulate emissions have larger uncertainties than the authors claim (i.e. Einstein coefficients, ozone concentration). Accounting for these uncertainties will significantly alter the results of this paper.

Further, the authors show that the applied OH model retrieves unrealistically high atomic oxygen and hydrogen in the MLT. Recent publications (s.f. Kaufmann et al. 2014, Mlynczak et al. 2018, Panka et al. 2018, and Zhu and Kaufmann 2018) have shown that [O] densities retrieved using SABER and SCIAMACHY measurements are much lower (by up to a factor 2 and more) than those retrieved in this study, specifically from 85-100 km. The model development (and the rate coefficient adjustments) must have a goal to reliably retrieve atmospheric properties from the observations. The very high [O] and [H] retrieved with the help of the new model indicates that there are still major flaws (it does not matter that it fits all selected emissions, this system has a very large number of unconstrained variables). The paper needs major revisions before making physical sense and being suitable for publication.
We lowered the total rate of OH(v=8)+O(3P) and checked the validity of our [O(3P)]. Taking into account the uncertainty of O(3P) derived here, our [O(3P)] results are now physically justified between 80 km and 95 km based on radiative and energetic constraints reported in Mlynczak et al. (2013b). The estimation of total [O(3P)] uncertainty was extended by additionally including uncertainty of SABER

O3 (~10 %; Smith et al., 2013), SABER temperature (3 %, Garcia-Comas et al., 2008) and SABER OH airglow emissions (6 %).
We also carried out sensitivity runs with different data sets of Einstein coefficients to test their impact on our results. As a consequence, the uncertainty of Einstein coefficients was increased from 10 % to 30 %.
We added an extended comparison of our model results with recent results presented by Mlynczak et al. (2018), Panka et al. (2018), and Zhu and Kaufmann (2018). We further explicitly stated that our [O(3P)] should be viewed as an upper limit in the altitude region above 87 km. However, despite that our [O(3P)] results are larger than the [O(3P)] in these three studies, our results are physically allowed, while conditions of chemical equilibrium of O3 are also valid. Additionally, we did not claim that our results are undeniable truth. But we think that our study makes justified assumptions which is still of value for publication.
A detailed response is presented below, when answering your specific comments.

Instead of fitting four emission bands while simultaneously retrieving [O] and [H] densities, I recommend for the revised study, to concentrate on retrieving [O] and [H] densities but only fit three emission bands (as will be discussed below, the OH(6-2) emission band is unreliable and taking into account its large uncertainty will alter the results of the current study).
We agree that SCIMACHY OH(6-2) VER is relatively noisy. But this issue was taken into account by the relatively large error bars of these measurements and even these relatively large uncertainties cannot explain all the differences of OH(6-2) VER between the Base model and SCIAMACHY measurements. Additionally, the major impact of OH(6-2) VER on our model results is the suggestion that OH($v\geq7$)+O2 primarily contribute to OH($v\leq5$)+O2.
However, the corresponding changes in the OH model do account for an increase of [O(3P)] and [H] of about 10 %. And the impact on the derived [O(3P)] profile also decreases with increasing altitude. The large [O(3P)] values above 90 km are primarily caused by different OH(v)+O3P rates and the assumed deactivation paths. Thus, we kept SCIAMACCHY OH(6-2) VER observations in our study.

Further, the authors must demonstrate how the rates derived from zonal mean profiles fit real single scans in three emission bands.
This was done in Sect. 3.4 (l. 593-618) where we analyzed the relation between [O(^{3}P)] and OH(9-7)+OH(8-6) VER presented in Fig. 7.

Specific comments:

Line 1.
The title states "New insights in OH airglow modelling…". The proposed new "insights" are highly speculative and are inconsistent with existing theory and experiments. The authors need to first show that reliable [O] and [H] can be derived when their OH model is applied before claiming any new insights.
The title was changed to: "Model results of OH airglow considering four different wavelength regions to derive night-time atomic oxygen and atomic hydrogen in the mesopause region"

In the introduction section, discussion regarding the current progress of [O] and [H] retrievals using SABER and SCIAMACHY instruments is missing. Retrieving these two parameters are a key point of this study and no background is given. Please cite recent [O] and [H] retrieval studies and their proper discussion.

We added (l. 100-117):

"The newly suggested rates of OH(ν)+O(^{3}P) were applied in different models to derive [O(^{3}P)] in the mesopause region. Mlynczak et al. (2018) used SABER OH airglow emissions observed at 2.0 µm to derive [O(^{3}P)] and assumed rates of 3.0×10^{-10} cm^3 s^{-1} and 1.5×10^{-10} cm^3 s^{-1} for OH(ν=9)+O(^{3}P) and OH(ν=8)+O(^{3}P), respectively. They further stated that deactivation of OH(ν=9)+O(^{3}P) has to occur via single-quantum quenching and that the OH(ν=8)+O_2 rate has to be smaller than known from laboratory measurements to get global annual energy budget into near balance. Panka et al. (2018) simultaneously investigated SABER OH airglow emissions measured at 2.0 µm and 1.6 µm, while applying faster rates for OH(ν=8)+O(^{3}P) and OH(ν)+O_2. Their [O(^{3}P)] values agree within the corresponding errors with the results reported by Mlynczak et al. (2018) above ~87 km but are larger in the altitude region below. The authors also demonstrated the high sensitivity of the derived [O(^{3}P)] from O(^{3}P) quenching rates applied in their model. Zhu and Kaufmann (2018) analyzed SCIAMACHY OH(9-6) transition. They used a value of 2.3×10^{-10} cm^3 s^{-1} for OH(ν=9)+O(^{3}P) which is lower than the one applied in the two previous studies, resulting in generally lower [O(^{3}P)] values in the altitude region above 87 km. Their rate for OH(ν=9)+O_2 lies between the corresponding rates of the two other studies, and consequently their [O(^{3}P)] is also between the [O(^{3}P)] values of these two studies below 87 km. Thus, recent publications indicate that the rate of OH(ν=9,8)+O(^{3}P) might be slower than previously suggested in Sharma et al. (2015). But this problem needs further attention because all three papers derive different [O(^{3}P)], depending on the data sets investigated."

Lines 205-216.

The retrieval of [O] and [H] are both dependent on the [O3] volume mixing ratio. The authors used nighttime [O3] taken from SABER.

The nighttime SABER [O3] has never been rigorously validated, nor is there a paper discussing its retrieval approach. Differences between WACCM and SABER [O3] are roughly a factor of 2 (Smith et al. 2014) and, therefore, one cannot rely on SABER [O3] as an input parameter.

Additionally, in Mlynczak et al. 2018, the conclusion is made that current SABER daytime [O3] and, supposedly, the nighttime one is too high based on a significantly lower [O] retrieved in that study. It is clear from equation 4a and 4b that any variation in [O3] will have a significant effect on [O] and [H]. For the revised study, I recommend using inputs taken from a self-consistent photochemical model like WACCM instead of ones taken from retrievals, which are not supported by any other studies. Additionally, uncertainties in the retrieved parameters due to large uncertainties in the [O3] must be estimated and discussed.

It is correct that chemistry-climate models like WACCM optimally contain descriptions of the state-of-the art of all known processes and usually provide a quite realistic representation of reality. However, these model results do not describe the "true" state of the atmosphere at any given point in time and space. Consequently, a comparison of models results and observations might be used to validate a model, but certainly not the observations.

In particular, WACCM has a well-known deficit of odd-oxygen, so it is not surprising that the WACCM O3 is less than SABER O3 or O3 obtained from any other measurement. This is a long-standing issue with WACCM and its predecessors. The daytime SABER O3 excess is certainly clear between 60 and 80 km. It may also be above that, but both Mlynczak et al. (2018) and Smith et al. (2014) could not conclude that above 80 km the daytime SABER O3 is too large.

The same is true for SABER night-time O3. Mlynczak et al. (2018) state that since "the cause of the larger daytime SABER ozone is not known, it is also possible that the SABER night O3 is also too large." This means that they cannot exclude an overestimation of their SABER night-time O3 because they do not know the reason behind SABER O3 daytime enhancement. But SABER night-time O3 might not have the same problem as SABER daytime O3. There are two candidates for the daytime O3 enhancement: One is the interfering bands of daytime CO2 that are not properly accounted for. Secondly, there might be an out-of-band light leak in the spectral filter. Even if it is an out of band leak, it may not be an issue at night-time.
Furthermore, recent comparison between MIPAS O3 and SABER O3 (Lopez-Puertas et al., 2018) did not show conclusive evidence that SABER night-time O3 is generally too large between 80 km and 100 km.
Thus, we think SABER night-time O3 inside the time-space interval of interest is not less reliable than any other data set and we did not replace SABER O3. The corresponding sentences in the paper were rephrased and an uncertainty of 10 % of SABER O3 (Smith et al., 2013) was assumed and included in the calculation of the total [O(3P)] uncertainty.

We added in the paper (l. 549-556):
"Recent comparisons between MIPAS O_3 and SABER O_3 derived at 9.6 µm were performed by Lopez-Puertas et al. (2018). The authors showed that night-time O_3 from SABER is slightly larger than night-time O_3 obtained from MIPAS in the altitude region 80-100 km over the equator (their Fig. 8 and 10) but these differences are within the corresponding errors. Thus, at least to our knowledge there is no conclusive evidence stating that SABER night-time O_3 is generally too large. Nevertheless, we considered an uncertainty of O_3 of about 10 % (Smith et al., 2013). The uncertainty of SABER temperature was estimated to be lower than 3 % (Garcia-Comas et al., 2008) while the total uncertainty of SABER OH(9-7)+OH(8-6) VER was assumed to be about 6 % (see Sect. 2.1.2)."

Lines 296-327.
"…we exclude the Einstein coefficients as a potential fundamental error source."
I do not agree with this statement. The new constraint imposed using the OH(6-2) emission band is unreliable. This band has a very small Einstein coefficient. The authors do not go into detail regarding the numerical differences among the literature of the OH(6-2) emission rate, but state that they are consistent.
The authors use the OH(6-2) coefficient taken from Xu et al. 2012 which is 1.767 sec-1. A more recent publication by Brooke et al. (2015) recalculated OH Einstein coefficients and found a rate of 1.16 sec-1 for the same transition. The rate of Xu et al. (2012) is approximately 50% larger than that of Brooke et al. (2015) and would significantly change the OH(6-2) emission profiles in Figures 1-5 as well as the results in Tables 2 and 3. The ab initio calculations of van der Loo and Groenenboom (2007, 2008) give values that are even smaller than Brooke et al. (2015) - the OH(6-2) emission rate of Xu et al. (2012) is 75% larger than that of van der Loo and Groenenboom (2007, 2008). Evidently, the issue of the OH Einstein coefficients is not yet settled.
The problem of all these data sets of Einstein coefficients is that the results strongly depend on how good the representation of the Hamiltonian for the OH molecule is which is used to solve the Schrödinger equation. It is expected that the calculations improve with time, but not necessarily at these large quanta changes. Multi quanta transitions of more than 2 quanta have small Einstein coefficients and are generally hard to model and calculate.
Also, it is inappropriate solely focusing on the Einstein coefficient of OH(6-2) because errors of this single transition might be partly compensated by errors of other OH transitions. However, we agree

with the referee that different Einstein coefficient data sets have to be taken into account before excluding them as a potential error source.

Thus, we carried out sensitivity runs and the results are displayed in Fig. 2 (see next page). We also rephrased and extended the corresponding section in the text as follows:
"Since the overestimation of the Base model is especially large for OH(6-2) VER, an impact of the Einstein coefficient of the corresponding transition must be considered. Regarding this aspect, we have to point out that studies based on HITRAN 2004 data set should be viewed more critically, because of erroneous OH transition probabilities. The Einstein coefficients used in this study were recently recalculated (Xu et al., 2012, their Table A1) and correspond to a temperature of 200 K, which is very close to mesopause temperature. Furthermore, these Einstein coefficients are consistent with the values of the HITRAN 2008 data set (Rothman et al., 2009). However, there are several other data sets of Einstein coefficients found in literature that might lead to different results. We therefore carried out sensitivity runs, using the Einstein coefficients reported by Turnbull and Lowe (1989), Nelson et al. (1990), van der Loo and Groenenboom (2007), Xu et al. (2012; =Base model), and Brooke et al. (2016). The corresponding results are presented in Figure 2 and show considerably large differences in case of OH(6-2) VER which are about a factor of 4 between the highest and lowest model output. In contrast, the individual simulations of OH(5-3)+OH(4-2) VER and OH(3-1) VER are rather consistent and vary only by ~10 %. These results emphasize that the choice of the Einstein coefficients is a potential error source for higher quanta transitions.
Regarding the credibility of the Einstein coefficients, it is generally assumed that the calculation improve with time. However, this is not necessarily true at quanta changes >2 because it all depends on how good the representation of the Hamiltonian for the OH molecule is, that is used to solve the Schrödinger equation. Multi quanta transitions >2 quanta have small Einstein coefficients and are generally hard to model and calculate. The assessment of the Einstein coefficients requires a detailed analysis of the corresponding calculations, which is beyond the scope of this study. We therefore cannot exclude the values used in the Base model as a potential error source, but we also think that our choice of the Einstein coefficients from Xu et al. (2012) is reasonable. Additionally, these values represent approximately the average model output of all five data sets considered here, while the model results based on Nelson et al. (1990) and van der Loo and Groenenboom (2007) represent the variability. Thus, we will not replace the Einstein coefficients by Xu et al. (2012) in our model but keep in mind that they might be too large.
Furthermore, the best agreement between the observations and the model was obtained by applying the Einstein coefficients reported by van der Loo and Groenenboom (2007). But even in this case, the model still overestimates the observations of all OH transitions in the altitude region between ~80 km and ~86 km. This pattern strongly supports the suggestion stated above that the rates and schemes associated with $OH(v)+O_2$ are incorrect."

We further added in the Conclusions (l. 635-637):
"Also note that the Einstein coefficients used here might be in error (see Sect.3.1; Fig. 2). This does not affect the two general conclusions drawn above but would impact the empirically derived rates."

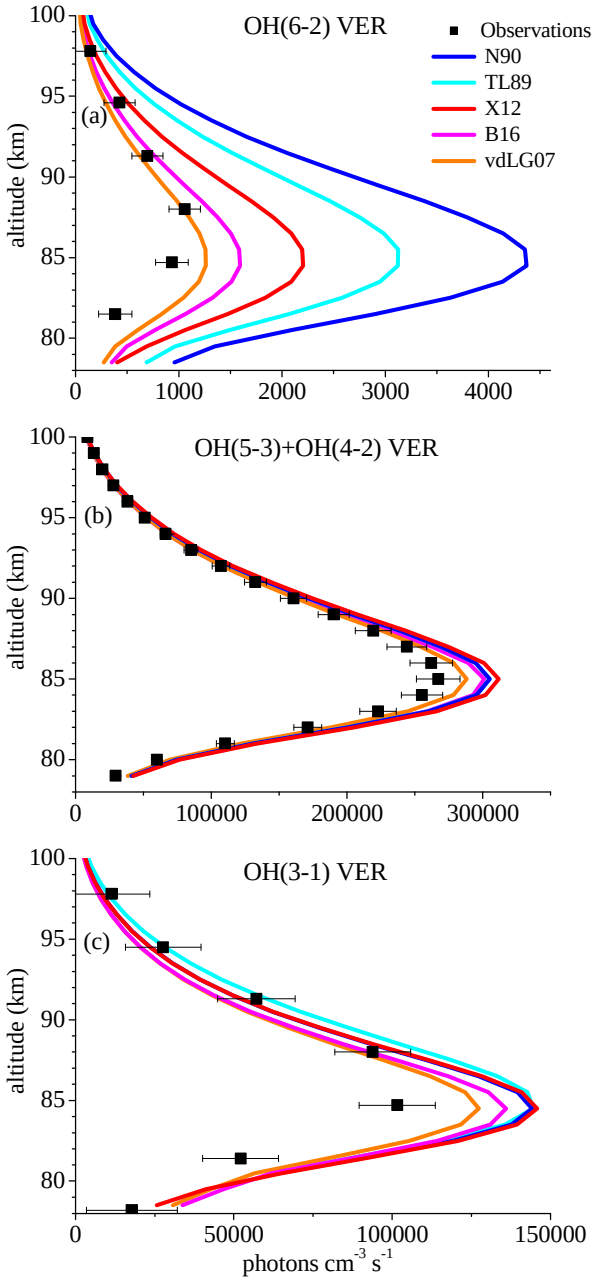

Figure 2 : Same as Figure 1 but for different sets of Einstein coefficients from literature, namely N90 (Nelson et al., 1990), TL89 (Turnbull and Lowe, 1989), X12 (=Base model; Xu et al., 2012), B16 (Brooke et al., 2016), and vdLG07 (van der Loo and Groenenboom, 2007).

To make matters worse, the SCIAMACHY OH(6-2) band displays a signal count two orders of magnitude smaller than that of the OH(3-1) band. The uncertainty of the VER signals for these two bands will be vastly different. Finally, because these two bands have a different Delta v and values of Einstein coefficients that are different by more than one order of magnitude, the uncertainty of the OH(6-2) band will be much larger.

Therefore, both the observed low VER signals and the large uncertainty in the value of the Einstein coefficient indicate knowledge of the OH(6-2) band is highly uncertain. As a result, the OH(6-2) emission band cannot be confidently used to constrain OH modeling parameters. For

manuscript revisions, I recommend to redo this study using only three OH emission bands. An alternative would be to validate the intensity of the OH(6-2) band by comparison with the OH(6-3) profile, which should be within the capabilities of SCIAMACHY.

We agree with the referee that SCIAMACHY OH(6-2) is relatively noisy but this was taken into account by the larger error bars presented in Fig. 1-5. These error estimates are based on the random noise at altitudes above the OH emission (l. 147-151) and we do not see any reason, why the OH(6-2) band should be omitted here because of low signal-to-noise ratio.

Additionally, including OH(6-2) does not considerably affect the [O(3P)] derived here (~10 %) and the impact also decreases with increasing altitude. However, based on the OH(6-2) emissions, we suggest that OH($v \geq 7$)+O2 primarily contribute to OH($v \leq 5$)+O2.

Thus, we did not exclude SCIAMACHY OH(6-2) from our study. Whether future studies will obtain similar results or strongly disagree with our suggestion cannot be known. But suggesting a new idea is not wrong even when based on relatively noisy data because these uncertainties were considered.

Lines 574-592.

"Applying their suggested limit, we found that in our case chemical equilibrium of O3 is probably true only above 80 km."

Recent studies have shown that the [O] and [H] retrieval approach used in this study may be flawed (Belikovich et al., 2018; Kulikov et al., 2017, 2018) and can introduce additional uncertainties. The authors addressed these issues very briefly here, but this needed to be more rigorously discussed. To say just simply "probably true" is insufficient. Additionally, uncertainties of the final results related to a probable chemical equilibrium breakdown need to be estimated and discussed.

This section was rearranged and extended as follows:

"The second aspect influencing the quality of the derived profiles is the assumption of chemical equilibrium of O_3, represented by Eq. (3). This issue was recently investigated by Kulikov et al. (2018), which carried out simulations with a 3-D chemical transport model and demonstrated that a wrongly assumed chemical equilibrium of O_3 may lead to considerable errors of derived [$O(^3P)$] and [H]. In order to test the validity of chemical equilibrium of O_3 locally, the authors suggested that OH(9-7)+OH(8-6) VER has to exceed $10 \times G \times B$, with *B* including several chemical reaction rates involving O_x and HO_x species. Note that this criterion requires simultaneously performed temperature and OH airglow measurements. Furthermore, this criterion is based on the assumption that the impact of atmospheric transport on chemical equilibrium of O_3 is negligible. Since our experiments fit these conditions, we applied their suggested limit and found that in our case chemical equilibrium of O_3 is valid above 80 km. We have to point out that the term "chemical equilibrium of O_3" refers to O_3 that does not deviate more than 10 % from O_3 in chemical equilibrium (Kulikov et al., 2018, their Eq. 2). Assuming that O_3 is always 10 % above or below O_3 in chemical equilibrium introduces an uncertainty of about 10 % at 80 km and 20 % at 95 km, additionally to the total uncertainty of [$O(^3P)$] and [H] estimated above. However, such a worst case scenario is rather unlikely while it is more realistic that O_3 actually varies around its chemical equilibrium concentration. Thus, an over- and underestimation of derived [$O(^3P)$] and [H] are assumed to compensate each other. Consequently, we conclude that the impact on the total uncertainty of [$O(^3P)$] and [H] due to deviations from chemical equilibrium of O_3 is negligible, but only because the previously used criterion is valid."

Lines 615-617.

"… we think that the O(3P) and H derived by the Best-fit model provides reasonable results between 80 and 95 km."

The [O] derived looks somewhat reasonable only below 87 km, but not above this altitude. At 95 km, the retrieved [O] is at least two times larger than Mlynczak et al. [2018] and more than a factor of 5 at 100 km. It has also been discussed in detail that high [O] will disrupt the energy balance in the MLT (Mlynczak et al. 2013, 2018) and influence temperature retrievals. If, in the revised study, the retrieved [O] and [H] remain high, then please demonstrate how it impacts the heating and cooling of MLT and discuss in detail possible ways to overcome the corresponding energy budget imbalance.

We compared our [O(3P)] derived here with the maximum [O(3P)] physically allowed by radiative constrains (Mlynczak et al., 2013b) and had to adjust our model to derive lower [O(3P)] values. This was done by reducing $k_{11}(v=8)$ from 2.3×10^{-10} cm^3 s^{-1} to 1.8×10^{-10} cm^3 s^{-1}. Now, our [O(3P)] matches the upper limit suggested by Mlynczak et al. (2013b) within the corresponding errors.

Thus, we added in the text (l. 474-486):

"At least to our knowledge, the total rate of $OH(v=8)+O(^3P)\rightarrow OH(v')+O(^1D)$ was not measured. Nevertheless, results reported by Mlynczak et al. (2018) and Panka et al. (2017, 2018) indicate that this rate might be slower than the value of 2.3×10^{-10} cm^3 s^{-1} suggested by Sharma et al. (2015). This is also in agreement with our findings here, because applying 2.3×10^{-10} cm^3 s^{-1} for $k_{11}(v=9,8)$ results in non-physical $[O(^3P)]$ values above 90 km. The corresponding value of $[O(^3P)]$ e.g. at 95 km is about 1.25 times larger than SABER $[O(^3P)]$ 2013 (Mlynczak et al., 2013a) which in turn is about 1.15 times larger than the upper limit of $[O(^3P)]$ (Mlynczak et al., 2013b, their Fig. 4). This results in a factor of $1.15\times1.25=1.44$ (=44 %) above the upper limit and cannot be explained by the uncertainty of the $[O(^3P)]$ profile derived here (40 %, see Sect. 3.4). In order to obtain reasonable $[O(^3P)]$ values, it was necessary to lower the rate of $k_{11}(v=8)$ to 1.8×10^{-10} cm^3 s^{-1}, and we therefore recommend $k_{11}(v=8)\leq1.8\times10^{-10}$ cm^3 s^{-1} as an upper limit to derive physically allowed $[O(^3P)]$ values."

Line 638-639.

"Furthermore, it cannot distinguish between OH(5) and OH(4) as a well as OH(9) and OH(8), and consequentially errors in OH(5) and OH(9) might be compensated by errors in OH(4) and OH(8) or vice versa".

This is a troubling statement as your main results in Table 3 (R11a, R11b, R11c, R11d, and R11g) involve these levels and describe rate coefficients for specific state-to-state reactions. This statement needs to be clarified. It sounds as if you treat OH(9)+OH(8) as a combined, single level as well as OH(5)+OH(4). Is this true? If you cannot distinguish between certain vibrational levels, then how can you determine rate coefficients for specific vibrational levels?

Yes, the SABER OH airglow emissions are a sum of OH(9-7) VER and OH(8-6) VER as well as OH(5-3) VER and OH(4-2) VER. We therefore cannot distinguish between OH(9) and OH(8) as well as OH(5) and OH(4).

However, when analyzing $OH(v=9)+O(^3P)\rightarrow OH(0\leq v'\leq v-5)+O(^1D)$, we can still draw some conclusion because this reaction can deactivate OH(v=9) only to $OH(v\leq4)$ but not OH(v=5). Thus, even if we cannot distinguish between OH(v=5) and OH(v=4) we can estimate a branching ratio of $OH(v=9)+O(^3P) \rightarrow OH(v=4)+O(^1D)$ if the total rate of $OH(v=9)+O(^3P) \rightarrow OH(v\leq4)+O(^1D)$ is known.

Furthermore, the rates of the individual paths presented in Table 3 are only a suggestion and not the main result. The main result of Table 3 is that the total loss rates of R11 are indicated to be slower compared to the values suggested by Sharma et al. (2015). These total rates presented here are a simplified solution in accordance with the rare laboratory experiments available and the OH transition considered. But as stated in the conclusion (l. 632-634): "Including additional OH transitions, …, might result in other values and deactivation schemes.

We rearranged this section as follows (l. 638-646):
“Furthermore, our OH airglow model is based on the transitions OH(9-7)+OH(8-6), OH(6-2), OH(5-3)+OH(4-2), and OH(3-1) only. Therefore, our model does not provide any information of OH(ν≤2). It further cannot distinguish between OH(ν=5) and OH(ν=4) as well as OH(ν=9) and OH(ν=8), respectively, and errors in OH(ν=5) and OH(ν=9) might be compensated by errors in OH(ν=4) and OH(ν=8) or vice versa. Consequently, the rates of the individual deactivation channels presented in Table 2 and Table 3 should be viewed as a suggestion only. But these issues will only be solved eventually when future laboratory experiments provide the corresponding OH(ν)+O_2 and OH(ν)+O(^{3}P) relaxation rates and deactivation channels. Nevertheless, we have to emphasize that the shortcomings of our model do not affect the two main conclusions drawn in this study.“

Tables 2 3. It is not clear if the results in Table 2 and 3 describe the Best-Fit model discussed in the conclusion. Table 2 shows empirically determined branching ratios of the OH(v) + O2 reaction for only VER observations “below 85 km” while Table 3 shows the branching ratios of the OH(v) + O(3P) reaction for only VER observations “above 85 km”. The lack of consistency adds confusion to the findings of this study. Please clarify this. Is there not a best-fit model for altitudes 80-100 km?
The individual model steps were always fit to the entire altitude interval 80-100 km. But OH(v)+O2 quenching is more important below 85 km while OH(v)+O(3P) becomes dominant above 85 km. Therefore, these altitudes were added in the caption of the tables.

But since this caused confusion we deleted “below 85 km” and “above 85 km” in the caption of Table 2 and 3.

Table 3.
The two most important processes (largest rate coefficients) estimated from the best fits are not energetically allowed! Processes R11a and R11c are highly endothermic processes by ~3000 cm-1 and 2000 cm-1, respectively.
The processes OH(ν=9)+O(3P)→OH(ν=4)+O(1D) and OH(ν=8)+O(3P)→OH(ν=3)+O(1D) are not findings of this study. They were adapted from OH(ν)+O(^{3}P)→OH(0≤ν’≤ν-5)+O(^{1}D) suggested by Sharma et al. (2015) and were also included in other OH airglow models (e.g. Panka et al., 2017, 2018). Therefore, for details about their credibility, we refer to Sharma et al. (2015, and references within).

Additionally, the state-to-state rate coefficients in Table 3 for the OH+O(3P) reaction appear to be in contradiction with the findings of Kalogerakis et al. (2016), who measured a large rate coefficient attributed to the resonant reaction OH(9)+O(3P)→OH(3)+O(1D). These results are non-physical and must be revised.
Kalogerakis et al. (2016) only reported that OH(ν=9)+O(3P)→OH(ν=3)+O(1D) is an important deactivation channel of OH(ν=9)+O(3P)→products. They did not provide any rate or branching ratio of the channel. To our understanding, “important” means “not negligible” but it does not mean “dominating”. Thus, we assumed that OH(ν=9)+O(3P)→OH(ν=3)+O(1D) has to occur but this channel is not necessarily the fastest deactivation path of OH(ν=9)+O(3P).

This was stated in the text (l. 490-493):
“However, not much is known about the individual branching ratios of R11 except that $OH(\nu=9)+O(^3P)\rightarrow OH(\nu=3)+O(^1D)$ is an important deactivation channel but not necessarily the dominating one (Kalogerakis et al., 2016).”

As stated above, it seems most likely that fitting the highly uncertain OH(6-2) signal that has large systematic errors have skewed the results of this paper. Removing this constraint may bring the revised OH model into better agreement with recent laboratory and modeling studies as well as retrieve reasonable [O] and [H].
As we wrote above, we took into account that OH(6-2) VER is a relatively noisy signal by considering the relatively large error bars. Also, OH(6-2) does not considerably affect derived [O(3P)] and [H] values (about 10 %).
Furthermore, we have to emphasize that, at least to our knowledge, the rates and deactivation schemes applied in the OH model are not in conflict with ANY laboratory measurements but partly disagree with other model studies. However, the intention of this study was not to match other model studies but to review recent rates and deactivation schemes, and consequently provide [O(3P)] and [H] values based on justified assumptions.

Figures 1-5.
Why are there no error bars displayed for the measured OH(5-3)+OH(4-2) VER emissions despite error bars displayed for the OH(6-2) and OH(3-1) emissions?
We added error bars of OH(5-3)+OH(4-2) VER in Fig.1-5 and a short description
as follows (l. 176-181):
“The total uncertainty of SABER OH airglow data used here comprises three different error sources. Since we used climatology of the measurements (see Sect. 2.2), there are sufficient samples that the random noise component of the total uncertainty is essentially zero. The remaining two major terms are the absolute calibration error (<5 %) and the “unfilter” factor error (<3 %). Assuming a root-sum-square propagation of the individual uncertainties, this results in a total uncertainty of about 6 % for all data points presented in this study.”

In general, the concept of fitting the zonal mean profiles for three OH bands is questionable. Operating with zonal mean profiles only, the authors are essentially fitting a single scenario (four individual signal scans). They must demonstrate how the rates derived from zonal mean profiles fit real single scans in measured emission bands. This will show whether the derived rates have any value for practical analysis of measurements of both instruments.
We used climatology instead of single scans because the individual scans are too noisy to derive any reliable rate coefficients. We are aware that deriving [O(3P)] and [H] based on zonal mean climatology instead of a scan-to-scan basis does introduce additional uncertainties. In particular, this approach fails when linearity between [O(3P)] and OH(9-7)+OH(8-6) VER breaks down.
But this issue was considered in Sect. 3.4 (l. 593-618; Fig. 7):
“The last problem lies in the fact that the approach used here (see Sect. 2.2) has to be applied to individual OH airglow profiles to derive $[O(^3P)]$ and [H] correctly. However, the individual scans of OH(6-2) were too noisy to analyze single profiles and we therefore used climatology for all input parameters. By investigating individual OH airglow profiles, we would derive individual $[O(^3P)]$ profiles and eventually average them to the mean $[O(^3P)]$ profile. While in our case, we directly derive the mean $[O(^3P)]$ profile. This makes no difference as long as the relation between OH airglow and

[$O(^3P)$] is a linear one. But Eq. (4b) shows that the relation between [$O(^3P)$] and OH(9-7)+OH(8-6) VER is only approximately linear because G also depends on [$O(^3P)$], as represented by the terms C_ν and $C_{\nu\nu'}$. The linearity between OH(9-7)+OH(8-6) VER and [$O(^3P)$] of an air parcel with a certain temperature and pressure is solely controlled by [$O(^3P)$]×G. Note that [H] too is affected by this non-linearity issue since [H] depends on G (Eq. (4a)). Thus, derived [H] values are only reliable as long as the derived [$O(^3P)$], and as a consequence G, is not seriously in error.
In order to test the linearity, [$O(^3P)$]×G was plotted as a function of [$O(^3P)$] and the corresponding results for Best fit model at five different heights are presented in Fig. 7. It is seen that the relation between [$O(^3P)$] and [$O(^3P)$]×G or OH(9-7)+OH(8-6) VER, respectively, is linear for small values of [$O(^3P)$], while a non-linear behaviour becomes more pronounced for larger values of [$O(^3P)$]. Furthermore, the starting point of the behaviour is shifted to lower [$O(^3P)$] values at higher altitudes. In order to estimate this threshold, we performed a visual analysis and determined an upper limit of [$O(^3P)$] before non-linearity of [$O(^3P)$]×G takes over. The approximated upper limits are added as dashed lines in Fig. 7. Finally, an [$O(^3P)$] value at a certain altitude is assumed to be true if this value is below the corresponding upper limit of [$O(^3P)$]. Otherwise, it should be viewed more critically. This was done for each altitude and we found that the [$O(^3P)$] and [H] profiles presented in Fig. 6 are plausible in the altitude region <95 km. In combination with the estimation of chemical equilibrium of O_3 and the maximum of physically allowed [$O(^3P)$], we think that the [$O(^3P)$] and [H] derived by the Best fit model are reasonable results between 80 km and 95 km. Note that these altitude limits do not affect the results with respect to OH(ν)+O_2 and OH(ν)+$O(^3P)$ presented in the Sect. 3.2 and 3.3."

Technical corrections:

Line 29-31.
This sentence needs a citation at the end.
Done, we added Andrews et al. (1987) and Mlynczak and Solomon (1993) as follows:
"Atomic oxygen in its ground state (O(3P)) and atomic hydrogen (H) strongly influence the energy budget in the mesopause region (~75-100 km) during day and night (Mlynczak and Solomon, 1993), and consequently affect atmospheric air temperature, wind, and wave propagation (Andrews et al., 1987)."

Lines 631-646.
These sentences should be moved to section 2.3: The OH airglow Base model.
We rearranged this section as follows (l. 629-642):
"We have to stress that we performed an empirical model study and the total rates and deactivation channels suggested here heavily depend on the OH transitions considered. Including additional OH transitions, like OH(9-4), OH(8-3), and OH(5-1) from the Optical Spectrograph and InfraRed Imager System (OSIRIS) on board the Odin satellite, might result in other values and deactivation schemes. This could be a subject of a future study. Also note that the Einstein coefficients used here might be in error (see Sect.3.1; Fig. 2). This does not affect the two general conclusions drawn above but would impact the empirically derived rates.
Furthermore, our OH airglow model is based on the transitions OH(9-7)+OH(8-6), OH(6-2), OH(5-3)+OH(4-2), and OH(3-1) only. Therefore, our model does not provide any information of OH(ν≤2). It further cannot distinguish between OH(ν=5) and OH(ν=4) as well as OH(ν=9) and OH(ν=8), respectively, and errors in OH(ν=5) and OH(ν=9) might be compensated by errors in OH(ν=4) and OH(ν=8) or vice versa. Consequently, the rates of the individual deactivation channels presented in

Table 2 and Table 3 should be viewed as a suggestion only. But these issues will only be solved eventually when future laboratory experiments provide the corresponding OH(ν)+O_2 and OH(ν)+O(^{3}P) relaxation rates and deactivation channels. Nevertheless, we have to emphasize that the shortcomings of our model do not affect the two main conclusions drawn in this study."

and added a shorter paragraph in Section 2.3 (l. 269-273):
"As described in the previous section, the OH airglow model is adjusted to fit OH(9-7)+OH(8-6) VER, OH(6-2) VER, OH(5-3)+OH(4-2) VER, and OH(3-1) VER. Thus, the model cannot provide information about OH($\nu \leq 2$). It further treats OH(ν=9) and OH(ν=8) as well as OH(ν=5) and OH(ν=4) as a single level and the corresponding deactivation channels should be viewed more critically. "

Model results of OH airglow considering four different wavelength regions to derive night-time atomic oxygen and atomic hydrogen in the mesopause region

Tilo Fytterer[1], Christian von Savigny[2], Martin Mlynczak[3], Miriam Sinnhuber[1]

[1]Institute for Meteorology and Climate Research, Karlsruhe Institute of Technology, Eggenstein-Leopoldshafen, 76344, Germany

[2]Institute of Physics, University of Greifswald, Greifswald, 17489, Germany

[3]NASA, Langley Research Center, Hampton, Virginia, 23681-2199, USA

Correspondence to: Miriam Sinnhuber (miriam.sinnhuber@kit.edu)

Abstract. Based on the zero dimensional box model CAABA/MECCA-3.72f, an OH airglow model was developed to derive night-time number densities of atomic oxygen ([O(^{3}P)]) and atomic hydrogen ([H]) in the mesopause region (~75-100 km). The profiles of [O(^{3}P)] and [H] were calculated from TIMED/SABER satellite OH airglow emissions measured at 2.0 µm. The two target species were used to initialize the OH airglow model, which was empirically adjusted to fit four different OH airglow emissions observed by the satellite/instrument configuration TIMED/SABER at 2.0 µm and at 1.6 µm as well as measurements by ENVISAT/SCIAMACHY of the transitions OH(6-2) and OH(3-1). Comparisons between the "Best fit model" obtained here and the satellite measurements suggest that deactivation of vibrationally excited OH(v) via OH(v≥7)+O_2 might favour relaxation to OH(v'≤5)+O_2 by multi-quantum quenching. It is further indicated that the deactivation pathway to OH(v'=v-5)+O_2 dominates. The results also provide general support of the recently proposed mechanism OH(v)+O(^{3}P)→OH(0≤v'≤v-5)+O(^{1}D) but suggest slower rates of OH(v=8,7,6,5)+O(^{3}P). Additionally, deactivation to OH(v'=v-5)+O(^{1}D) might be preferred. The profiles of [O(^{3}P)] and [H] derived here are plausible between 80 km and 95 km but should be regarded as an upper limit. The values of [O(^{3}P)] obtained in this study agree with the corresponding TIMED/SABER values between 80 km and 85 km, but are larger from 85 to 95 km due to different relaxation assumptions of OH(v)+O(^{3}P). The [H] profile found here is generally larger than TIMED/SABER [H] by about 50 % from 80 to 95 km, which is

Gelöscht: New insights into

Gelöscht: modelling

Gelöscht: A

Gelöscht: from satellite OH airglow observations

Gelöscht: . T

Gelöscht: is based on the zero dimensional box model CAABA/MECCA-3.72f and

Gelöscht: 30-35

primarily attributed to our faster OH(ν=8)+O_2 rate.

Gelöscht: might be

Gelöscht: attributed to too high O_3 night-time values

1 Introduction

Atomic oxygen in its ground state ($O(^3P)$) and atomic hydrogen (H) strongly influence the energy budget in the mesopause region (~75-100 km) during day and night (Mlynczak and Solomo, 1993), and consequently affect atmospheric air temperature, wind, and wave propagation (Andrews et al., 1987). Therefore, an improved knowledge of the abundance of $O(^3P)$ and H is of great importance when studying the mesopause region. At these altitudes, $O(^3P)$ has a direct impact on the heating rates by participating in several exothermic chemical reactions (Mlynczak and Solomon, 1993, their Table 4). But $O(^3P)$ also contributes to radiative cooling by exciting CO_2 via collisions, leading to increased infrared emissions of CO_2 and partly opposing the $O(^3P)$ chemical heating effect. Night-time H plays a crucial role in the mesopause region due to the destruction of ozone (O_3) which is accompanied by the release of a considerable amount of heat (Mlynczak and Solomon, 1993). This chemical reaction additionally leads to the production of vibrationally excited hydroxyl radicals (OH(ν≥0)) up to the vibrational level ν=9, causing the formation of OH emission layers in the atmosphere (Meinel bands; Meinel, 1950).

Direct measurements of $O(^3P)$ and H are relatively rare because as atomic species they do not have observable vibration-rotation spectra. Consequently, measuring these species in the mesopause region by remote sensing requires complex methods while in situ observations are rather expensive (e.g. Mlynczak et al., 2004; Sharp and Kita, 1987). Thus, there exists no global data set based on direct observations. As a consequence, an indirect method was introduced by Good (1976) to derive $[O(^3P)]$ and [H] during night, using OH airglow emissions. This approach was also adapted by Mlynczak et al. (2013a; 2014; 2018) which derived a global data set of night-time $[O(^3P)]$ and [H] in the mesopause region from satellite observations of OH(ν). The method is based on the assumption of chemical steady state of O_3 and further depends on several radiative lifetimes, chemical reactions, and physical processes involving OH(ν). However, the corresponding total rate coefficients and branching ratios are still not sufficiently known, and thus present a large source of uncertainty in the derivation of $[O(^3P)]$

and [H].

There are two major issues currently discussed in the literature which considerably affect the overall abundance of derived $O(^3P)$ and H. The first problem addresses the underlying deactivation schemes of $OH(v)$ from the higher excited state v to the lower excited state v' ($v'<v$) by collisions with O_2. This can generally occur via sudden death ($OH(v)+O_2 \rightarrow OH(v'=0)+O_2$), single-quantum ($OH(v)+O_2 \rightarrow OH(v'=v-1)+O_2$), or multi-quantum ($OH(v)+O_2 \rightarrow OH(v'<v)+O_2$) quenching. However, in case of the sudden death approach, it is still unknown where such a huge amount of excess energy is transferred. The second crucial point comprises the deactivation scheme and the total rate of $OH(v)+O(^3P)$, including the new pathway $OH(v)+O(^3P) \rightarrow OH(0 \leq v' \leq v-5)+O(^1D)$ suggested by Sharma et al. (2015).

Over the last three to four decades, several model studies attempted to fit OH airglow measurements, using different rates and schemes for the deactivation of $OH(v)$ by O_2 and by $O(^3P)$. And at least to our knowledge, there is no general agreement about which model is correct. The deactivation of $OH(v)$ by O_2 in many models (e.g. von Savigny et al., 2012; Mlynczak et al., 2013a; Grygalashvyly et al., 2014; Panka et al., 2017) is based on the model proposed by Adler-Golden (1997). It assumes a combination of multi-quantum and single-quantum quenching and was derived from theoretical considerations and ground-based observations. Xu et al. (2012) investigated measurements from the Sounding of the Atmosphere using Broadband Emission Radiometry (SABER) instrument on board the NASA Thermosphere-Ionosphere-Mesosphere Energetics and Dynamics (TIMED) satellite of the OH airglow emissions at 2.0 µm and at 1.6 µm. Their results support the model of Adler-Golden (1997) but suggest slower total $OH(v)+O_2$ rates. They further exclude the sudden death mechanism as a possible deactivation scheme. There are also two theoretical studies (Shalashilin et al., 1995; Caridade et al., 2002) which investigated $OH(v)$ deactivation via O_2, both supporting a combination of multi-quantum and single-quantum quenching similar to the model of Adler-Golden (1997).

However, Russell and Lowe (2003) and Russell et al. (2005) analyzed OH(8-3) and $O(^1S)$ airglow emissions measured by the Wind Imaging Interferometer (WINDII) instrument on board the Upper Atmospheric Research Satellite (UARS). Both airglow emissions were used to derive separate data sets of $[O(^3P)]$ and the best agreement between these two $[O(^3P)]$ data sets was obtained when a sudden

Gelöscht: of

Gelöscht: individually

Gelöscht: profiles

death scheme for OH(ν)+O_2 quenching was applied. Kaufmann et al. (2008) investigated several OH airglow spectra between 1 µm and 1.75 µm measured by the Scanning Imaging Absorption Spectrometer for Atmospheric Chartography (SCIAMACHY) instrument on board the Environmental Satellite (ENVISAT). They found best agreement between their model and the measured OH airglow spectra when a combination of sudden death and single-quantum quenching was used.

Vibrationally dependent rates of OH(ν)+O(^{3}P) were determined by Varandas (2004) and Caridade et al. (2013), using quasi-classical trajectory calculations. Their results suggest that deactivation occurs via a chemical reaction as well as multi-quantum quenching. Kalogerakis et al. (2011) obtained a deactivation rate of OH(ν=9)+O(^{3}P) from laboratory experiments which is several times larger than the rate from these calculations. But applying this fast quenching rate led to non-physical [O(^{3}P)] values and associated heating rates (Smith et al., 2010; Mlynczak et al., 2013a). Thus, Sharma et al. (2015) proposed a new mechanism OH(ν)+O(^{3}P)→OH(0≤ν'≤ν-5)+O(^{1}D) to account for results from both theory and experiment. Very recent laser experiments and model studies support this new pathway while the exact values of the branching ratios and total loss rates are still not known (Kalogerakis et al., 2016; Panka et al., 2017). However, recently published results by Mlynczak et al. (2018) oppose this mechanism. They also applied the new rate of Kalogerakis et al. (2011) for OH(ν=9)+O(^{3}P). But in order to get the annual energy budget into near balance, it was necessary to assume that at least OH(ν=9)+O(^{3}P) occurs via single-quantum relaxation. Additionally, the rate of OH(ν=8)+O_2 had to be reduced and is considerably smaller than the value reported from Adler-Golden (1997).

The newly suggested rates of OH(ν)+O(^{3}P) were applied in different models to derive [O(^{3}P)] in the mesopause region. Mlynczak et al. (2018) used SABER OH airglow emissions observed at 2.0 µm to derive [O(^{3}P)] and assumed rates of 3.0×10^{-10} cm^3 s^{-1} and 1.5×10^{-10} cm^3 s^{-1} for OH(ν=9)+O(^{3}P) and OH(ν=8)+O(^{3}P), respectively. They further stated that deactivation of OH(ν=9)+O(^{3}P) has to occur via single-quantum quenching and that the OH(ν=8)+O_2 rate has to be smaller than known from laboratory measurements to get global annual energy budget into near balance. Panka et al. (2018) simultaneously investigated SABER OH airglow emissions measured at 2.0 µm and 1.6 µm, while applying faster rates for OH(ν=8)+O(^{3}P) and OH(ν)+O_2. Their [O(^{3}P)] values agree within the corresponding errors with the

results reported by Mlynczak et al. (2018) above ~87 km but are larger in the altitude region below. The authors also demonstrated the high sensitivity of the derived [$O(^3P)$] from $O(^3P)$ quenching rates applied in their model. Zhu and Kaufmann (2018) analyzed SCIAMACHY OH(9-6) transition. They used a value of 2.3×10^{-10} cm^3 s^{-1} for $OH(v=9)+O(^3P)$ which is lower than the one applied in the two previous studies, resulting in generally lower [$O(^3P)$] values in the altitude region above 87 km. Their rate for $OH(v=9)+O_2$ lies between the corresponding rates of the two other studies, and consequently their [$O(^3P)$] is also between the [$O(^3P)$] values of these two studies below 87 km. Thus, recent publications indicate that the rate of $OH(v=9,8)+O(^3P)$ might be slower than previously suggested in Sharma et al. (2015). But this problem needs further attention because all three papers derive different [$O(^3P)$], depending on the data sets investigated.

In order to address the two major issues stated above, this paper is focused on the development of a zero dimensional box model for atmospheric OH airglow with the intention to derive night-time [$O(^3P)$] and [H] in the mesopause region. The model considers the formation of OH(v) via $H+O_3$ and deactivation of OH(v) due to spontaneous emission of photons, chemical reactions and physical collisions with atmospheric air compounds N_2, O_2, and $O(^3P)$. We used the indirect method introduced by Good (1976) and derived night-time [$O(^3P)$] and [H] from TIMED/SABER OH emissions at ~2.0 µm, while also considering the OH airglow observations from TIMED/SABER at ~1.6 µm as well as the OH(6-2) and OH(3-1) transitions measured by ENVISAT/SCIAMACHY. Further sensitivity runs were carried out to estimate the uncertainty on the derived values of [$O(^3P)$] and [H] due to the different deactivation schemes, overall rate constants, and branching ratios.

2 Data and method

2.1 Satellite measurements

2.1.1 ENVISAT/SCIAMACHY

The SCIAMCHY instrument (Bovensmann et al., 1999) was an 8-channel spectrometer on board ENVISAT, providing atmospheric OH airglow emission measurements between ~220 nm and ~2380

nm. ENVISAT was launched into a polar and sun-synchronous orbit and crossed the equator at ~10 LT and ~22 LT. The ENVISAT mission started in March 2002 and SCIAMACHY was nearly continuously operating until the end of the mission in April 2012 caused by a spacecraft failure. The SCIAMACHY instrument performed measurements in different observations modes, including night-time (~22 LT) limb scans over the tangent altitude range ~75-150 km. These measurements are only available throughout the year at latitudes between the equator and 30° N.

In this paper, we used SCIAMACHY level 1b data v7.04 to retrieve OH airglow volume emission rates (VERs) of the OH(3-1) and OH(6-2) bands in the wavelength ranges of 1515-1546 nm and 837.5-848.0 nm, respectively. The retrieval approach applied here is very similar to the one described in von Savigny et al. (2012). The retrieval does not cover the complete spectra of the OH(3-1) and OH(6-2) bands, and consequently a "correction factor" of 2.48 for OH(3-1) VER and 2.54 for OH(6-2) VER was added to account for the entire band emissions at mesopause temperature. The data set further includes corrections for misalignments and other measurement errors (Gottwald et al., 2007). Investigations performed by Bramstedt et al. (2012) showed a drift of the SCIAMACHY tangent height of less than 20 m $year^{-1}$ which is negligible for our study.

The uncertainties of the OH(3-1) VER and OH(6-2) VER retrievals from SCIAMACHY limb observations correspond to the propagated uncertainties of the observed limb emission rate (LER) profiles. The latter are estimated from the LER values in the tangent height range between 110 km and 150 km, where the actual atmospheric emissions should be zero. The VER uncertainties are first determined for daily and zonally averaged data. The uncertainties used in this analysis correspond to the mean uncertainties averaged over all days with co-located SCIAMACHY and SABER observations.

2.1.2 TIMED/SABER

The SABER instrument (Russell et al., 1999) on board the TIMED satellite has been nearly continuously operating since January 2002, collecting over 98 % of all possible data. The instrument scans the atmosphere from the surface up to altitudes of ~400 km while providing a vertical resolution of about 2 km throughout the entire height interval. Due to the geometry of the satellite orbit and the regular yaw manoeuvres every ~60-65 days, SABER only provides complete coverage of the latitude

range between ~55° S and ~55° N. The SABER instrument measures the OH VERs at ~2.0 µm and at ~1.6 µm which approximately corresponds to the transitions of OH(9-7)+OH(8-6) and OH(5-3)+OH(4-2), respectively. The contribution of OH(7-5) to OH VER at 2.0 µm and of OH(3-1) to OH VER at 1.6 µm is only about a few percents (Xu et al., 2012; Mlynczak et al., 2013a) and is neglected in this paper.

In this study, we used the SABER Level 2A data v2.0 of the "unfiltered" OH VERs at 2.0 µm and at 1.6 µm, the air temperature and pressure, and the volume mixing ratios (VMRs) of O_3 (derived at 9.6 µm). There are also SABER O_3 measurements at 1.27 µm but these observations are not available during night. New night-time VMRs of O(^{3}P) and H (Mlynczak et al., 2018) were used for comparison with the results derived from our model. The "unfilter" factor applied to OH VER adjusts the originally measured OH VER by the SABER instrument to the total VER emitted by OH in the corresponding vibrational bands, while considering the shape, width, and transmission of the SABER broadband filters (Mlynczak et al., 2005). Outliers were excluded by screening the data as suggested by Mlynczak et al. (2013a). The SABER data used here were further restricted to observations between 21 LT and 23 LT to approximately match the SCIAMACHY measurement time at ~22 LT. In order to be consistent with the naming of the SCIAMACHY OH airglow observations, the SABER OH airglow at 2.0 µm and at 1.6 µm are referred to as OH(9-7)+OH(8-6) and as OH(5-3)+OH(4-2) throughout the paper.

The total uncertainty of SABER OH airglow data used here comprises three different error sources. Since we used climatology of the measurements (see Sect. 2.2), there are sufficient samples that the random noise component of the total uncertainty is essentially zero. The remaining two major terms are the absolute calibration error (<5 %) and the "unfilter" factor error (<3 %). Assuming a root-sum-square propagation of the individual uncertainties, this results in a total uncertainty of about 6 % for all data points presented in this study.

2.2 Method

In order to minimize uncertainties between SABER and SCIAMACHY due to different measurement characteristics, we focused on the latitude range from 0° to 10° N, which was covered by both instruments throughout the entire year. A broader latitude band is not recommended because SABER and SCIAMACHY do not uniformly cover the same latitudes, leading to disagreements between the

Gelöscht: issues

real latitude of the observations and the nominal latitude of the interval. The accepted profiles of both instruments within the chosen latitude interval were averaged to zonal mean nightly mean values. All these zonal mean nightly means from January 2003 to December 2011 were used to calculate a climatology, including only days on which both SCIAMACHY and SABER data are available.

The approach to derive [O(^{3}P)] and [H] applied here was developed by Good (1976) and is described in detail in Mlynczak et al. (2013a). Thus, we only give a brief summary here. The measured SABER OH(9-7)+OH(8-6) VER (photons cm^{-3} s^{-1}) is given by Eq. (1):

$$\mathrm{OH(9-7)+OH(8-6)\ VER} = k_1[\mathrm{H}][\mathrm{O_3}]G(f_v, A_{vv'}, C_{vv'}), \qquad (1)$$

where k_1 is the rate constant of the chemical reaction H+O$_3$, representing direct production. The function G (Eq. (2)) comprises all relevant production and loss processes of OH(9-7) VER and OH(8-6) VER:

$$G = \frac{f_9}{A_9 + C_9} A_{97} + \frac{f_8}{A_8 + C_8} A_{86} + \frac{f_9}{A_9 + C_9} \frac{A_{98} + C_{98}}{A_8 + C_8} A_{86}, \qquad (2)$$

The subscripts v and v' ($v'<v$) are the vibrational states of OH before and after the corresponding process. The terms f_v are the nascent distributions and describe the production efficiency of OH(v) via the reaction H+O$_3$. Total radiative loss due to spontaneous emissions is considered by the Einstein coefficients A_v (s^{-1}) which are the inverse radiative life times of OH(v). The total loss rate C_v (s^{-1}) is the sum of loss due to collisions with the air compounds (N$_2$, O$_2$, O(^{3}P)), including chemical reactions and physical quenching. The terms $A_{vv'}$ and $C_{vv'}$ represent the specific state-to-state transitions.

In the second step, chemical equilibrium of O$_3$ during night is assumed as follows:

$$k_1[\mathrm{H}][\mathrm{O_3}] + k_2[\mathrm{O(^3P)}][\mathrm{O_3}] = k_3[\mathrm{O(^3P)}][\mathrm{O_2}][\mathrm{M}], \qquad (3)$$

meaning that O$_3$ loss due to H and O(^{3}P) (left side) is balanced by O$_3$ formation via the three-body-reaction O(^{3}P)+O$_2$+M (right side). Here, k_2 and k_3 are the corresponding rate constants of O(^{3}P)+O$_3$ and O(^{3}P)+O$_2$+M, respectively, while M being an air molecule and [M] being the total number density of the air.

Gelöscht: is

Finally, rewriting Eq. (1) enables the derivation of [H] while [O(^{3}P)] is calculated by substituting Eq. (3) in Eq. (1) and rewriting the resulting term as follows:

$$[\mathrm{H}] = \frac{\mathrm{OH}(9-7) + \mathrm{OH}(8-6)\ \mathrm{VER}}{\mathrm{G}\, k_1 [\mathrm{O_3}]}, \qquad (4a)$$

$$[\mathrm{O}(^3\mathrm{P})] = \frac{\mathrm{OH}(9-7) + \mathrm{OH}(8-6)\ \mathrm{VER}}{\mathrm{G}\,(k_3 [\mathrm{O_2}][\mathrm{M}] - k_2 [\mathrm{O_3}])}. \qquad (4b)$$

Air temperature and air pressure from SABER were used to calculate [M], [O_2] (VMR of 0.21), and [N_2] (VMR of 0.78) as well as to convert SABER O_3 VMR into [O_3] via the ideal gas law. The chemical reaction rates and physical quenching processes involved are described in Sect. 2.3. The values of [$O(^3P)$] and [H] were individually derived for each altitude. Finally, the obtained vertical profiles of [$O(^3P)$] and [H] were used to initialize the OH airglow model (see Sect. 2.3).

It is apparent from Eq. (4a-b) that any changes applied to the input parameters (G, O_2, O_3, M, k_1, k_2, k_3) are balanced by the derived values of [$O(^3P)$] and [H], without assuming any a priori information of [$O(^3P)$] and [H]. In contrast, OH(9-7)+OH(8-6) VER is not affected by the input parameters and therefore identical in every model run. However, the goal of this paper is to develop a model which does not only fit OH(9-7)+OH(8-6) VER observations but also reproduces the three other airglow measurements OH(6-2) VER, OH(5-3)+OH(4-2) VER, and OH(3-1) VER. We have to further point out, that the relation between [$O(^3P)$] and OH(9-7)+OH(8-6) VER is not linear since the function G also depends on [$O(^3P)$], as represented by the terms C_v and $C_{vv'}$. In fact, Eq. (4b) is a quadratic expression with respect to [$O(^3P)$] but treated here as a linear one, making no substantial differences for small [$O(^3P)$]. Nevertheless, this issue is addressed in detail in Sect. 3.4.

2.3 The OH airglow Base model

The model used in this study is based on the atmospheric chemistry box model Module Efficiently Calculating the Chemistry of the Atmosphere/Chemistry As A Box model Application (MECCA/CAABA-3.72f; Sander et al., 2011). The box model calculates the temporal evolution of chemical species inside a single air parcel of a certain pressure and temperature, making the model well suited for sensitivity studies. The CAABA/MECCA standard model was extended by several chemical reactions and physical quenching processes involving OH(v) which are described in this section. The model was run until it reaches steady-state, defined by the agreement between the measured and

Gelöscht: *M* as well as the number densities of

Gelöscht: , and

Gelöscht: very

modelled OH(9-7)+OH(8-6) VER.

The OH airglow model described in this section is referred to as “Base model” because it is the starting point of our model studies. But we have to point out that there is no such a thing as a commonly accepted OH airglow base model in the literature. The Base model takes into account all major formation and loss processes of OH(v) (Table 1) which are commonly used in other models in the literature and are assumed not to be seriously in error. The model comprises the production of OH(v) via the chemical reaction $H+O_3$ as well as the deactivation due to spontaneous emission and the removal physical quenching and chemical reactions with N_2, O_2, and $O(^3P)$.

The chemical reactions $H+O_3$, $O(^3P)+O_3$, and $O(^3P)+O_2+M$ were already included in the CAABA/MECCA standard model and their corresponding rates were taken from the latest Jet Propulsion Laboratory (JPL) report 18 (Burkholder et al., 2015). The reaction $H+O_3$ can populate OH(v) at all vibrational level v≤9 and the nascent distribution of OH(v) was taken from Adler-Golden (1997). The spontaneous emissions are given by the Einstein coefficients at 200 K (Xu et al., 2012). Deactivation of OH(v) by N_2 is assumed to occur via single-quantum quenching. The rates at room temperature for OH(v≤8) and for OH(v=9) were taken from Adler-Golden (1997) and Kalogerakis et al. (2011), respectively.

Quenching of OH(v) by O_2 is based on the values reported by Adler-Golden (1997, their Table 3) which comprise a combination of multi-quantum and single-quantum quenching. However, Adler-Golden (1997) applied a factor of ~1.5 to account for mesopause temperature based on comparisons between laboratory measurements at room temperature of OH(v=8)+O_2 and the corresponding rate inferred from OH(8-3) rocket observations in the mesopause region. But later experiments reported by Lacousiere et al. (2003) and calculations by Caridade et al. (2002) suggest smaller values. The latter study further indicates that the temperature dependence decreases for lower vibrational levels and becomes negligible for OH(v≤4). Consequently, the rates presented in Adler-Golden (1997) were scaled to room temperature measurements (v=1-6 Dodd et al., 1991; v=7 Knutsen et al., 1996; v=8 Dyer et al., 1997; v=9 Kalogerakis et al., 2011), and afterwards a factor of 1.1 for OH(v≥6) and 1.05 for OH(v=5) was applied.

Gelöscht: s

Gelöscht: up to the

Gelöscht: added

The removal of OH(v) via collisions with $O(^3P)$ is included by using a combination of multi-quantum quenching (Caridade et al., 2013, their Table 1) and chemical reactions (Varandas, 2004). The rates were obtained from quasi-classical trajectory calculations at 210 K, approximately matching mesopause temperature.

As described in the previous section, the OH airglow model is adjusted to fit OH(9-7)+OH(8-6) VER, OH(6-2) VER, OH(5-3)+OH(4-2) VER, and OH(3-1) VER. Thus, the model cannot provide information about OH(v≤2). It further treats OH(v=9) and OH(v=8) as well as OH(v=5) and OH(v=4) as a single level and the corresponding deactivation channels presented in Table 2 and 3 should be viewed more critically.

3 Results and discussions

Figure 1 displays vertical profiles of a) OH(6-2) VER, b) OH(5-3)+OH(4-2) VER, and c) OH(3-1) VER, comparing the observations (black squares) with the corresponding Base model output (red line). The model results of OH(6-2) VER and OH(3-1) VER are a 4 km running average to take the averaging kernels of SCIAMACHY measurements into account. The Base model approximately matches the general shape of the measured profiles but overestimates the three OH airglow measurements at the altitude of maximum VER. A closer look at the relative differences shows that the ratio model/observation at the altitude of maximum VER is about 2.0, 1.2, and 1.3 for OH(6-2), OH(5-3)+OH(4-2), and OH(3-1), respectively. Furthermore, these ratios increase with decreasing altitude, indicating that the overestimation of the Base model might be associated with O_2 quenching.

The differences between Base model and observations are quite substantial in case of OH(6-2) VER. This implies a general problem of the rates or schemes included in the Base model, requiring a detailed error analysis. The focus was set on potential error sources of OH(6-2) VER because the relative differences between model and measurements are largest compared to the other two OH transitions, and secondly because changes of OH(v=6) will affect the lower vibrational levels, but not vice versa.

3.1 Potential error sources of OH(6-2) VER in the Base model

Based on the results presented in Fig. 1, the potential error source has to have an effect on the entire

height interval and must have a stronger impact on OH(6-2) compared to the other two OH transitions. We further focus on quantities with large uncertainties. For the latter reason, temperature is excluded as possible source because to account for a reduction of OH(6-2) VER by a factor of 2, temperature must be increased by more than 20 K (not shown here). Such a large error is very unlikely considering that a zonal mean climatology (2003-2011) is used here.

Since the overestimation of the Base model is especially large for OH(6-2) VER, an impact of the Einstein coefficient of the corresponding transition must be considered. Regarding this aspect, we have to point out that studies based on HITRAN 2004 data set should be viewed more critically, because of erroneous OH transition probabilities. The Einstein coefficients used in this study were recently recalculated (Xu et al., 2012, their Table A1) and correspond to a temperature of 200 K, which is very close to mesopause temperature. Furthermore, these Einstein coefficients are consistent with the values of the HITRAN 2008 data set (Rothman et al., 2009). However, there are several other data sets of Einstein coefficients found in literature that might lead to different results. We therefore carried out sensitivity runs, using the Einstein coefficients reported by Turnbull and Lowe (1989), Nelson et al. (1990), van der Loo and Groenenboom (2007), Xu et al. (2012; =Base model), and Brooke et al. (2016). The corresponding results are presented in Figure 2 and show considerably large differences in case of OH(6-2) VER which are about a factor of 4 between the highest and lowest model output. In contrast, the individual simulations of OH(5-3)+OH(4-2) VER and OH(3-1) VER are rather consistent and vary only by ~10 %. These results emphasize that the choice of the Einstein coefficients is a potential error source for higher quanta transitions.

Regarding the credibility of the Einstein coefficients, it is generally assumed that the calculation improve with time. However, this is not necessarily true at quanta changes >2 because it all depends on how good the representation of the Hamiltonian for the OH molecule is, that is used to solve the Schrödinger equation. Multi quanta transitions >2 quanta have small Einstein coefficients and are generally hard to model and calculate. The assessment of the Einstein coefficients requires a detailed analysis of the corresponding calculations, which is beyond the scope of this study. We therefore cannot exclude the values used in the Base model as a potential error source, but we also think that our choice of the Einstein coefficients from Xu et al. (2012) is reasonable. Additionally, these values represent

approximately the average model output of all five data sets considered here, while the model results based on Nelson et al. (1990) and van der Loo and Groenenboom (2007) represent the variability. Thus, we will not replace the Einstein coefficients by Xu et al. (2012) in our model but keep in mind that they might be too large.

Furthermore, the best agreement between the observations and the model was obtained by applying the Einstein coefficients reported by van der Loo and Groenenboom (2007). But even in this case, the model still overestimates the observations of all OH transitions in the altitude region between ~80 km and ~86 km. This pattern strongly supports the suggestion stated above that the rates and schemes associated with OH(v)+O_2 are incorrect.

Gelöscht: , Turnbull and Lowe (1989) after the correction suggested by Adler-Golden (1997) is applied, and Nelson et al. (1990) which are applied to derive new night-time and from SABER (Mlynczak et al., 2018). Therefore, an error of a factor of 2 for the transition of OH(6-2) is rather unlikely. Consequently, we exclude the Einstein coefficients as a potential fundamental error source.

The nascent distribution of the excited OH states of the chemical reaction H+O_3 was observed in several studies and all of them agree that OH(v) is primarily formed in the vibrational levels v=8 and v=9 (e.g. Charters et al., 1971; Streit and Johnston, 1976; Ohoyama et al., 1985; Klenerman and Smith, 1987). The values used in the Base model were taken from Adler-Golden (1997) which are based on measurements reported by Charters et al. (1971) and agree with values obtained by Klenerman and Smith (1987) and Streit and Johnston (1976). The values found by Ohoyama et al. (1985) show some differences, but according to Klenerman and Smith (1987), their results are fundamentally flawed. This also affects the nascent distribution used by Mlynczak and Solomon (1993) which is an average of Charters et al. (1971), Ohoyama et al. (1985), and Klenerman and Smith (1987).

Therefore, we think that our nascent distribution used here is likely not a serious error source. However, minor errors might be introduced by extrapolating the nascent distribution to lower vibrational levels as it was done for the values used in our study (Adler-Golden, 1997). It is also possible that part of the nascent value of OH(v=6) is not due to direct production via H+O_3 but results from contributions of OH(v≥7). In order to test the potential impact of the OH(v=6) nascent value on OH(6-2) VER, we assumed an extreme scenario by reducing the OH(v=6) nascent value from 0.03 to zero. But the corresponding results of OH(6-2) VER of the Base model run (not shown here) are only about 15 % lower compared to the values presented in Fig. 1. Further sensitivity runs also showed that an increase of the ratio f_9/f_8 is associated with a decrease of modelled OH(6-2) VER but even the extreme case of f_9=1 and f_8=0 could not account for a factor of 2. Note that changes of the overall rate constant of H+O_3

affect all considered OH transitions in a similar way, Thus, we conclude that direct production of OH(v) is unlikely to be the reason for the overestimation of OH(6-2) VER by the Base model.

The physical removal of OH(v) by N_2 is included as single-quantum relaxation which is supported by theoretical studies (Shalashilin et al., 1992; Adler-Golden, 1997). Assuming a sudden death scheme with the same overall deactivation rates resulted in a decrease of simulated OH(6-2) VER by less than 10 % at the altitude of maximum VER. The total deactivation rate for OH(v=9) used here is about 1.5 times higher than the one suggested by Adler-Golden (1997) but the difference between the corresponding model OH(6-2) VERs is negligible (<1 %). There are two studies reporting temperature dependence of N_2 quenching (Shalashilin et al., 1992; Burtt and Sharma, 2008), both agreeing with measurements at room temperature. However, the calculations of the former study imply slower quenching rates at mesopause temperature compared to their respective values at room temperature whereas the latter publication indicates the opposite behaviour, reporting a ratio between the rate at 200 K and 300 K of approximately 1.7 for OH(v=8) and 1.3 for OH(v=9). These factors are generally supported by López-Puertas et al. (2004) which applied an empirically determined factor of 1.4 to the rates of Adler-Golden (1997) to account for mesopause temperature. Since the temperature dependence is still uncertain, we tested both possibilities. We increased and decreased the overall OH(v)+N_2 quenching rates by a factor of 1.5 which led to higher or lower OH(6-2) VERs by about 5 %. Therefore, N_2 is too inefficient as a OH(v) quenching partner to cause differences of OH(6-2) VER of a factor of 2.

The overall rate and exact pathways of OH(v)+O(^{3}P) are also still not known well enough but O(^{3}P) has nearly no influence on OH(v) at altitudes below 85 km. It therefore cannot be the only reason for the differences presented in Fig. 1. Consequently, deactivation by O_2 is the only remaining candidate which has a crucial influence on OH(v) throughout the entire height interval. Therefore, we will first focus on OH(v)+O_2 (Sect. 3.2) before investigating a potential influence of O(^{3}P) on OH(v) in Sect. 3.3.

3.2 Deactivation of OH(v) by O_2

The overestimation of OH(6-2) VER by the Base model can be generally corrected either by slower rates of OH(v=9,8,7)+O_2 or by a faster rate of OH(v=6)+O_2. The overall deactivation of OH(v=9) was measured by Chalamala and Copeland (1993) and they recommended a value of 2.1×10^{-11} cm^3 s^{-1}. This

result was later confirmed by Kalogerakis et al. (2011), reporting a rate of 2.2×10^{-11} cm^3 s^{-1}. The rates for OH(v=8,7,6)+O_2 are each based on a single study only (v=8 Dyer et al., 1997; v=7 Knutsen et al., 1996; v=6 Dodd et al., 1991). But at least to our knowledge, there are no signs that the rates of OH(v=9,8,7,6)+O_2 are fundamentally flawed. In order to test the impact of the individual rates on OH(6-2) VER, we carried out sensitivity runs by varying the overall rates within their recommended 2σ errors. Thus, we reduced the values of OH(v=9,8,7)+O_2 to 16×10^{-12} cm^3 s^{-1}, 7×10^{-12} cm^3 s^{-1}, and 5×10^{-12} cm^3 s^{-1}, respectively, while the rate of OH(v=6)+O_2 was increased to 4.5×10^{-12} cm^3 s^{-1}. But even under this favoured condition, the Base model output of OH(6-2) VER decreased only by a factor of 1.5, still not close to the required difference of a factor of 2. Additionally, the assumed scenario is rather unlikely since the overall rates were obtained by independent studies.

The possibility of a systematic offset of OH(v≤6)+O_2 rates, which are based on the single study (Dodd et al., 1991), is also excluded because of the very good agreement of this OH(v=2)+O_2 rate with the value obtained by Rensberger et al. (1989). Furthermore, when we increased the OH(v≤6)+O_2 rates by a factor of 3, the Base model approximately fits OH(6-2) VER and OH(3-1) VER but underestimates OH(5-3)+OH(4-2) VER by more than 30 %. Temperature dependence also affects the O_2 deactivation rates used here. But the factor to account for mesopause region temperature is suggested to be lower than 1.3 (Lacousiere et al., 2003; Cadidade et al., 2002) which has a weaker impact on OH(6-2) VER than the scenarios considered above.

Consequently, when applying the standard deactivations rates and schemes found in the literature, neither errors of the overall rates nor uncertainties of the temperature dependence can give a reasonable explanation of the overestimation of OH(6-2) VER Base model output shown in Fig. 1a. Since the overall rates were actually measured while the deactivation schemes are solely based on theoretical considerations, it is more convincing that the potential error source lies within OH(v)+O_2 deactivation scheme rather than in the deactivation rates.

Gelöscht: probably

In order to considerably reduce OH(6-2) VER, we assumed an extreme scenario and substituted the multi-quantum relaxation (OH(v)+O_2→OH(v'<v)+O_2) in the Base model by a sudden death (OH(v)+O_2→OH+O_2) approach. This new model is referred to as "O_2 SD model" and the

corresponding results are displayed in Fig. 3 as red lines, showing that the simulated OH(6-2) VER matches the observations within the error bars below 85 km and above ~92 km. The model still overestimates the measurements in the altitude region ~90 km, which might be related to O(^{3}P) quenching (see Sect. 3.3). The O_2 SD model output for the other two OH transitions (Fig. 3b-c) is clearly too low, implying that OH(v)+O_2 quenching cannot occur via sudden death alone. We also conclude that the contribution of higher excited states OH(v≥7) to OH(v=6) must be negligible or even zero and these higher states are suggested to primarily populate lower vibrational levels OH(v≤5). Therefore, OH(v)+O_2 has to occur via multi-quantum quenching because in case of single-quantum deactivation the contribution of OH(v≥7) to OH(v=6) is considerably larger than zero.

According to Finlayson-Pitts and Kleindienst (1981), OH(v) might be relaxing to v'=v-5 while the excess energy is transferred to form $O_2(b^1\Sigma)$. This vibration-to-electronic energy transfer was also mentioned by Anlauf et al. (1968) and is supported by the close energy match of the transition from OH(v=9) to OH(v=4) and from $O_2(X^3\Sigma)$ to $O_2(b^1\Sigma)$ of about 36.6 kcal mol^{-1} and 37.5 kcal mol^{-1}, respectively. Although there is no experimental support of this deactivation pathway, this approach gives a reasonable explanation for the observed pattern in our study and OH(v) as a potential source of excited O_2, as discussed in Howell et al. (1990) and Murtagh et al. (1990). However, evaluating whether the product is really $O_2(b^1\Sigma)$ or another excited O_2 state is beyond the scope of this study. Thus, we concluded that deactivation of OH(v) by O_2 has to satisfy the following condition:

OH(v≥6)+O_2 → OH(v'≤5)+O_2 (R8)

while we further assume that the pathway

OH(v≥6)+O_2 → OH(v'=v-5)+O_2 (R9)

is the preferred deactivation channel.

In order to test whether R9 could be the only pathway of R8 we assumed multi-quantum relaxation via:

OH(v)+O_2 → OH(v-5)+O_2 (R10a)

or OH(v)+O_2 → OH(v-4)+O_2 (R10b).

If R10a is integrated in the model (Fig. 3b-c, O_2 v-5 model), the corresponding model output at altitudes <90 km is only about 10 % below the observations of OH(5-3)+OH(4-2) VER and approximately

Gelöscht: 2
Gelöscht: above
Gelöscht: 2
Gelöscht: w
Gelöscht: 0≤
Gelöscht: v-
Gelöscht: 2

matches OH(3-1) VER measurements within the error bars. The underestimation of the OH(5-3)+OH(4-2) VER measurements by the model could be attributed to minor errors of the OH(ν)+O_2 overall rates in combination with a slightly different OH(ν) branching of H+O_3. Therefore, we cannot completely rule out R10a as a possible solution, even if there are still some differences between the modelled and the observed OH VER. Replacing R10a by R10b in the model (Fig. 3b-c, O_2 ν-4 model) results in an overestimation of the observations of OH(5-3)+OH(4-2) VER and OH(3-1) VER by about 20 % to 30 %, and consequently this assumption is not further considered as a potential solution.

The results shown in Fig. 3 suggest that the OH airglow model is not able to reproduce the three OH airglow observations when sudden death or simplified multi-quantum schemes for OH(ν)+O_2 are applied. But the O_2 ν-5 model output is quite close to the measurements, suggesting that R9 might be the dominating deactivation channel within a multi-quantum relaxation scheme in accordance with R8. We therefore included these two conditions in the so-called "O_2 best fit model" and the results are displayed in Fig. 4. The corresponding branching ratios for the individual pathways are summarized in Table 2.

The simulated OH airglow fits well with the three OH airglow observations within the error bars below 85 km. In the altitude region above 85 km, it is seen that the model still overestimates OH(6-2) VER while OH(3-1) VER is indicated to be slightly underestimated. Furthermore, this pattern is not seen in OH(5-3)+OH(4-2) VER and therefore could be attributed to deviations due to the different satellite/instrument configurations between TIMED/SABER and ENVISAT/SCIAMACHY. But since this behaviour only occurs in the upper part of the vertical profiles and is not seen throughout the entire height interval, it is more likely related to O(^{3}P) quenching.

3.3 Deactivation of OH(ν) by O(^{3}P)

Only recently, Sharma et al. (2015) proposed a new pathway of OH(ν)+O(^{3}P) by providing a direct link between higher and lower vibrational levels via:

OH(ν)+O(^{3}P) → OH(0≤ν'≤ν-5)+O(^{1}D) (R11),

with the vibrationally independent reaction constant $k_{11} = 2.3\times10^{-10}$ cm^3 s^{-1}. While the value of k_{11}(ν=9) is based on measurements (Kalogerakis et al., 2011; Thiebaud et al., 2010) and on calculations

Gelöscht: Including
Gelöscht: b
Gelöscht: 2
Gelöscht: 2
Gelöscht: 3

(Varandas, 2004), the values for $k_{11}(v=5, 6, 7, 8)$ are only assumed to be identical to $k_{11}(v=9)$ and should be viewed more critically.

We adapted R11 in the "O_2 best fit $O(^3P)$ v-5 model" in such a way that the product is OH(v'=v-5)+$O(^1D)$ and the results obtained are displayed as blue lines in Fig. 5. Comparisons for OH(6-2) VER in Fig. 5a show an underestimation of the model at altitudes >85 km. A sensitivity study was carried out that showed that the impact of OH(v=9,8,7)+$O(^3P)$ on OH(6-2) VER is negligible. This is reasonable because these three upper states only indirectly influence OH(6-2) via R11. Consequently, our analysis suggests a lower value of $k_{11}(v=6)$ and best agreement between model output and OH(6-2) VER observations was obtained for an overall rate of approximately 0.8×10^{-10} cm^3 s^{-1}.

In case of OH(5-3)+OH(4-2) VER, presented in Fig. 5b, the new approach leads to a weak underestimation of the observations by the model in the altitude region above 85 km, even if OH(v=9)+$O(^3P)$ of R11 solely populates OH(v=4). The model results are most sensitive to $k_{11}(v=5)$, and therefore this rate might be too fast. Considering our best fit value obtained for $k_{11}(v=6)$, it is indicated that $k_{11}(v)$ decreases with decreasing vibrational level and this feature is discussed below in more detail. Thus, an upper limit of $k_{11}(v=5)<k_{11}(v=6)$ is recommended and the actual rate coefficient has to balance the direct contribution of OH(v=9) to OH(v=4) via R11. Investigating another scenario of $k_{11}(v=5)$ being zero showed that the branching of OH(v=9) to OH(v=4) has to be at least about 0.6 which corresponds to a rate of a ~1.4×10^{-10} cm^3 s^{-1}.

The assumption that $k_{11}(v)$ decreases at lower vibrational levels is supported by the overall rate of OH(v=7)+$O(^3P)\rightarrow$OH(v')+$O(^1D)$ at mesopause temperature which is suggested to be on the order of $0.9\text{-}1.6\times10^{-10}$ cm^3 s^{-1} (Thiebaud et al., 2010; Varandas, 2004). At least to our knowledge, the total rate of OH(v=8)+$O(^3P)\rightarrow$OH(v')+$O(^1D)$ was not measured. Nevertheless, results reported by Mlynczak et al. (2018) and Panka et al. (2017, 2018) indicate that this rate might be slower than the value of 2.3×10^{-10} cm^3 s^{-1} suggested by Sharma et al. (2015). This is also in agreement with our findings here, because applying 2.3×10^{-10} cm^3 s^{-1} for $k_{11}(v=9,8)$ results in non-physical $[O(^3P)]$ values above 90 km. The corresponding value of $[O(^3P)]$ e.g. at 95 km is about 1.25 times larger than SABER $[O(^3P)]$ 2013 (Mlynczak et al., 2013a) which in turn is about 1.15 times larger than the upper limit of $[O(^3P)]$

Gelöscht: 4
Gelöscht: 4
Gelöscht: which
Gelöscht: implied
Gelöscht: seems
Gelöscht: 4
Gelöscht: high
Gelöscht: This

(Mlynczak et al., 2013b, their Fig. 4). This results in a factor of 1.15×1.25=1.44 (=44 %) above the upper limit and cannot be explained by the uncertainty of the [O(^{3}P)] profile derived here (40 %, see Sect. 3.4). In order to obtain reasonable [O(^{3}P)] values, it was necessary to lower the rate of k_{11}(v=8) to 1.8×10^{-10} cm^3 s^{-1}, and we therefore recommend k_{11}(v=8)≤1.8×10^{-10} cm^3 s^{-1} as an upper limit to derive physically allowed [O(^{3}P)] values.

It is seen in Fig. 5c that observations and O_2 best fit O(^{3}P) v-5 model output of OH(3-1) VER are in agreement within the corresponding measurement errors but the model values seem to be slightly too low at heights >85 km. In this altitude region, simulated OH(3-1) VER is most influenced by OH(v=9,8)+O(^{3}P) of R11 because both vibrational levels can directly populate OH(v=3). However, not much is known about the individual branching ratios of R11 except that OH(v=9)+O(^{3}P)→OH(v=3)+O(^{1}D) is an important deactivation channel but not necessarily the dominating one (Kalogerakis et al., 2016). This agrees with our results presented here because the O_2 best fit O(^{3}P) v-5 model only considers a contribution of OH(v=8) to OH(v=3) and the underestimation indicated in Fig. 5c could be attributed to the missing channel OH(v=9)+O(^{3}P)→OH(v=3)+O(^{1}D). The conclusions drawn from comparisons between three different airglow observations and our model studies with respect to OH(v)+O(^{3}P) quenching are summarized in Table 3.

Finally, all these findings presented in Table 2 and 3 were adapted in the “Best fit model” (Fig. 5, red lines), resulting in an overall agreement between model output and measurements within the corresponding errors. Note that k_{11}(v=7) used here is the average of the lower and upper limits derived from Thiebaud et al. (2010) and Varandas (2004) which is unlikely to be seriously in error. Furthermore, we have to point out that lowering k_{11}(v=8) does only impact the [O(^{3}P)] and [H] derived here but does not affect the general conclusions drawn in this section.

The empirically determined solution presented here implies that the contribution of OH(v=9) to OH(v=8) via quenching with O(^{3}P) is close to zero (see Table 1 and this section). In contrast, the model described in Mlynczak et al. (2018) assumes single-quantum relaxation (OH(v=9)+O(^{3}P)→OH(v=8)+O(^{3}P)) to get the global annual energy budget into near balance. But applying this approach in our OH model (same total rate of 3×10^{-10} cm^3 s^{-1} and varying the rates for

Gelöscht: Thus, an upper limit of $k_{11}(5)<k_{11}(6)$ is recommended and the actual rate coefficient has to balance the direct contribution of OH(9) to OH(4) via R11. Investigating another scenario of $k_{11}(5)$ being zero showed that the branching of OH(9) to OH(4) has to be at least about 0.6 which corresponds to a rate of a ~1.4×10^{-10} cm^3 s^{-1}.

Gelöscht: 4

Gelöscht: 4

Gelöscht: 4

Gelöscht: it is indicated that the value of $k_{11}(8)$ might be lower than 2.3×10^{-10} cm^3 s^{-1} which can be assumed based on the other rates of k_{11}(v). But we did not find any study reporting an observed $k_{11}(8)$ rate, and consequently we did not change $k_{11}(8)$. Besides,

OH(v≤8)+O(^{3}P)) leads to a considerable overestimation of OH(6-2) VER. Additionally, the shape of simulated OH(5-3)+OH(4-2) VER slightly mismatches the observed OH(5-3)+OH(4-2) VER above 90 km (not shown here). Based on these sensitivity runs, we conclude that at least part of OH(v=9)+O(^{3}P) channel has to be deactivated via multi-quantum quenching. This is supported by the results presented by Panka et al. (2017) which adjusted an OH airglow model to fit night-time $CO_2(\nu_3)$ emissions at 4.3 µm. However, this study reported empirically determined rates for OH(5≤v≤8)+O(^{3}P) generally higher than the rates obtained in this work. But these differences might be attributed to their faster values of OH(v)+O_2 because they seem to have falsely assumed that the rates of Adler-Golden (1997) do not take mesopause temperature into account. Thus, we think that their rates of OH(v)+O_2 are too high, at least by a factor of ~1.5. Since they performed an empirical study, it is not possible to estimate how much this issue affects the rates of OH(5≤v≤8)+O(^{3}P). But we know from our work that higher rates of OH(v)+O_2 lead to higher values of OH(6-2) VER, OH(5-2)+OH(4-2) VER, and OH(3-1) VER which can be generally balanced by higher rates of OH(5≤v≤8)+O(^{3}P). Considering our comparisons with these two studies, we think that the rates of OH(v)+O(^{3}P) should be investigated in more detail in future studies as this rate has a huge impact on derived values of [O(^{3}P)] (Panka et al., 2018).

3.4 Derived profiles of [O(^{3}P)] and [H]

Figure 6 displays the vertical profiles of [O(^{3}P)] and [H] obtained by the Best fit model in comparison with the results derived from SABER OH(9-7)+OH(8-6) VER only (Mlynczak et al., 2018). The [O(^{3}P)] profiles seen in Fig. 6a agree below 85 km but the Best fit model shows gradually larger values in the altitude region above. These larger values are caused by the different deactivation rates and schemes of OH(v)+O(^{3}P), agreeing with general pattern reported in Panka et al. (2018). We have to point out that other studies (e.g. von Savigny and Lednyts'kyy, 2013) observed a pronounced [O(^{3}P)] maximum of about 8×10^{11} cm^{-3} at 95 km. The [O(^{3}P)] derived here indeed shows similar values at 95 km but a maximum is not seen. Nevertheless, the [O(^{3}P)] in our study obtained above 95 km looks rather unexpected and possible reasons are discussed below.

The night-time [H] derived in this study shows similar pattern as SABER [H], including the maximum at 80 km. But Best fit model [H] is systematically larger than SABER [H] by a factor of approximately

Gelöscht: 5

Gelöscht: 5

Gelöscht: higher

1.5. This is primarily caused by our faster OH(v=8)+O_2 rate compared to the rate applied in Mlynczak et al. (2018). Similar to the comparisons with [$O(^3P)$], Best fit model [H] results also shows unexpected patterns above 95 km.

The quality of the derived profiles is primarily affected by three different uncertainty sources. The first source includes uncertainties due to the rates of chemical and physical processes as well as the background atmosphere considered in the Best fit model. We assessed the 1σ uncertainty by assuming uncorrelated input parameters. Adler-Golden (1997) did not state any uncertainties for f_9 and f_8 but these values should be similar to the uncertainty of f_8 derived by Klenerman and Smith (1987). Therefore, we applied an uncertainty of 0.03 for f_9 and f_8. In case of the Einstein coefficient, we adapted an uncertainty of 30 %, which is based on the five sets of Einstein coefficients analyzed in Sect. 3.1. Note that larger uncertainties only occur for multi quanta transitions >2 quanta. But [$O(^3P)$] and [H] were calculated from the transition OH(9-7)+OH(8-6) where the agreement is better. All the other 1σ uncertainties of the input parameters were taken from their respective studies.

Recent comparisons between MIPAS O_3 and SABER O_3 derived at 9.6 µm were performed by Lopez-Puertas et al. (2018). The authors showed that night-time O_3 from SABER is slightly larger than night-time O_3 obtained from MIPAS in the altitude region 80-100 km over the equator (their Fig. 8 and 10) but these differences are within the corresponding errors. Thus, at least to our knowledge there is no conclusive evidence stating that SABER night-time O_3 is generally too large. Nevertheless, we considered an uncertainty of O_3 of about 10 % (Smith et al., 2013). The uncertainty of SABER temperature was estimated to be lower than 3 % (Garcia-Comas et al., 2008) while the total uncertainty of SABER OH(9-7)+OH(8-6) VER was assumed to be about 6 % (see Sect. 2.1.2). The total 1σ uncertainty was obtained by calculating the root-sum-square of all individual uncertainties. The results of 1σ uncertainty of [$O(^3P)$] and [H] derived by the Best fit model are shown as error bars in Fig. 6. The error bars of SABER [$O(^3P)$] and [H] were adapted from the corresponding publication.

In case of the Best fit model [$O(^3P)$] profile, the 1σ uncertainty varies between 30 % and 40 %, depending on altitude. The individual contributions of the input parameters to the total 1σ uncertainty are considerably different. Einstein coefficients and nascent distribution each account for about 10 %

Gelöscht: might be partly caused by too

Gelöscht: high O_3 night-time values, as suggested by Mlynczak et al. (2018).

Gelöscht: 1

Gelöscht: as suggested by Mlynczak et al. (2013).

Gelöscht: 5

Gelöscht: 20

Gelöscht: 30

and 5 %, respectively, throughout the entire height interval. The influence of the collision rates is about 5 % and gradually decreases to zero with increasing altitude. In contrast, the chemical reaction rates k_2 and k_3 account for ~80 % to ~85 % of the overall 1σ uncertainty of the derived $[O(^3P)]$ profiles. The total 1σ uncertainty of [H] varies between 25 % and 40 % with k_1 being the major uncertainty source (~80 %) below 85 km. In higher altitude regions, the impact due to uncertainty of $[O(^3P)]$ becomes gradually more important and both k_1 and $[O(^3P)]$ each contribute close to one half to the overall uncertainty at altitudes >95 km. We further assumed a worst case scenario (not shown here), meaning that all uncertainties of the input parameters contribute to either higher or lower $[O(^3P)]$ values, obtaining a worst case 1σ uncertainty of approximately 80 % for $[O(^3P)]$ and about 65 % for [H]. However, it is more likely that the uncertainties are uncorrelated since they originate from independent measurements.

The second aspect influencing the quality of the derived profiles is the assumption of chemical equilibrium of O_3, represented by Eq. (3). This issue was recently investigated by Kulikov et al. (2018), which carried out simulations with a 3-D chemical transport model and demonstrated that a wrongly assumed chemical equilibrium of O_3 may lead to considerable errors of derived $[O(^3P)]$ and [H]. In order to test the validity of chemical equilibrium of O_3 locally, the authors suggested that OH(9-7)+OH(8-6) VER has to exceed 10×G×B, with *B* including several chemical reaction rates involving O_x and HO_x species. Note that this criterion requires simultaneously performed temperature and OH airglow measurements. Furthermore, this criterion is based on the assumption that the impact of atmospheric transport on chemical equilibrium of O_3 is negligible. Since our experiments fit these conditions, we applied their suggested limit and found that in our case chemical equilibrium of O_3 is valid above 80 km. We have to point out that the term "chemical equilibrium of O_3" refers to O_3 that does not deviate more than 10 % from O_3 in chemical equilibrium (Kulikov et al., 2018, their Eq. 2). Assuming that O_3 is always 10 % above or below O_3 in chemical equilibrium introduces an uncertainty of about 10 % at 80 km and 20 % at 95 km, additionally to the total uncertainty of $[O(^3P)]$ and [H] estimated above. However, such a worst case scenario is rather unlikely while it is more realistic that O_3 actually varies around its chemical equilibrium concentration. Thus, an over- and underestimation of derived $[O(^3P)]$ and [H] are assumed to compensate each other. Consequently, we conclude that the

Gelöscht: lower than 6
Gelöscht: 5
Gelöscht: 90
Gelöscht: also
Gelöscht: 20
Gelöscht: 30
Gelöscht: 5
Gelöscht: 6
Gelöscht: 5
Gelöscht: 0
Gelöscht: They suggested that chemical equilibrium of O_3 is only valid when
Gelöscht: exceeds a certain threshold, depending
Gelöscht: on *G* and
Gelöscht: Applying their
Gelöscht: , we
Gelöscht: probably true only

impact on the total uncertainty of [O(^{3}P)] and [H] due to deviations from chemical equilibrium of O_3 is negligible, but only because the previously used criterion is valid.

The last problem lies in the fact that the approach used here (see Sect. 2.2) has to be applied to individual OH airglow profiles to derive [O(^{3}P)] and [H] correctly. However, the individual scans of OH(6-2) were too noisy to analyze single profiles and we therefore used climatology for all input parameters. By investigating individual OH airglow profiles, we would derive individual [O(^{3}P)] profiles and eventually average them to the mean [O(^{3}P)] profile. While in our case, we directly derive the mean [O(^{3}P)] profile. This makes no difference as long as the relation between OH airglow and [O(^{3}P)] is a linear one. But Eq. (4b) shows that the relation between [O(^{3}P)] and OH(9-7)+OH(8-6) VER is only approximately linear because G also depends on [O(^{3}P)], as represented by the terms C_ν and $C_{\nu\nu}$. The linearity between OH(9-7)+OH(8-6) VER and [O(^{3}P)] of an air parcel with a certain temperature and pressure is solely controlled by [O(^{3}P)]×G. Note that [H] too is affected by this non-linearity issue since [H] depends on G (Eq. (4a)). Thus, derived [H] values are only reliable as long as the derived [O(^{3}P)], and as a consequence G, is not seriously in error.

In order to test the linearity, [O(^{3}P)]×G was plotted as a function of [O(^{3}P)] and the corresponding results for Best fit model at five different heights are presented in Fig. 7. It is seen that the relation between [O(^{3}P)] and [O(^{3}P)]×G or OH(9-7)+OH(8-6) VER, respectively, is linear for small values of [O(^{3}P)], while a non-linear behaviour becomes more pronounced for larger values of [O(^{3}P)]. Furthermore, the starting point of the behaviour is shifted to lower [O(^{3}P)] values at higher altitudes. In order to estimate this threshold, we performed a visual analysis and determined an upper limit of [O(^{3}P)] before non-linearity of [O(^{3}P)]×G takes over. The approximated upper limits are added as dashed lines in Fig. 7. Finally, an [O(^{3}P)] value at a certain altitude is assumed to be true if this value is below the corresponding upper limit of [O(^{3}P)]. Otherwise, it should be viewed more critically. This was done for each altitude and we found that the [O(^{3}P)] and [H] profiles presented in Fig. 6 are plausible in the altitude region <95 km. In combination with the estimation of chemical equilibrium of O_3 and the maximum of physically allowed [O(^{3}P)], we think that the [O(^{3}P)] and [H] derived by the Best fit model are reasonable results between 80 km and 95 km. Note that these altitude limits do not affect the results with respect to OH(v)+O_2 and OH(v)+O(^{3}P) presented in the Sect. 3.2 and 3.3.

Gelöscht: 6

Gelöscht: 6

Gelöscht: 5

Gelöscht: provides

4 Conclusions

We presented a zero dimensional box model which fits the VER of four different OH airglow observations, namely TIMED/SABER OH(9-7)+OH(8-6) and OH(5-3)+OH(4-2) as well as ENVISAT/SCIAMACHY OH(6-2) and OH(3-1). Based on a night-time mean zonal mean climatology of co-location measurements between 2003 and 2011 at 0°-10° N, we found that I) $OH(v)+O_2$ is likely to occur via multi-quantum deactivation while $OH(v\geq7)$ primarily contribute to $OH(v\leq5)$ and might prefer deactivation to $OH(v'=v-5)+O_2$. This relaxation scheme generally agrees with results reported in Russell et al. (2005) but is considerably different to the commonly used scheme suggested by Adler-Golden (1997). We further found II) general support for the new pathway $OH(v)+O(^3P)\rightarrow OH(v')+O(^1D)$ proposed by Sharma et al. (2015) but suggest slower total loss rates of $OH(v=8,7,6,5)+O(^3P)$. Additionally, hints for a favoured deactivation to $OH(v'=v-5)+O(^1D)$ are obtained.

We have to stress that we performed an empirical model study and the total rates and deactivation channels suggested here heavily depend on the OH transitions considered. Including additional OH transitions, like OH(9-4), OH(8-3), and OH(5-1) from the Optical Spectrograph and InfraRed Imager System (OSIRIS) on board the Odin satellite, might result in other values and deactivation schemes. This could be a subject of a future study. Also note that the Einstein coefficients used here might be in error (see Sect.3.1; Fig. 2). This does not affect the two general conclusions drawn above but would impact the empirically derived rates.

Furthermore, our OH airglow model is based on the transitions OH(9-7)+OH(8-6), OH(6-2), OH(5-3)+OH(4-2), and OH(3-1) only. Therefore, our model does not provide any information of $OH(v\leq2)$. It further cannot distinguish between OH(v=5) and OH(v=4) as well as OH(v=9) and OH(v=8), respectively, and errors in OH(v=5) and OH(v=9) might be compensated by errors in OH(v=4) and OH(v=8) or vice versa. Consequently, the rates of the individual deactivation channels presented in Table 2 and Table 3 should be viewed as a suggestion only. But these issues will only be solved eventually when future laboratory experiments provide the corresponding $OH(v)+O_2$ and $OH(v)+O(^3P)$ relaxation rates and deactivation channels. Nevertheless, we have to emphasize that the shortcomings of

Gelöscht: But we have to emphasize that our OH airglow model is based on the transitions OH(9-7)+OH(8-6), OH(6-2), OH(5-3)+OH(4-2), and OH(3-1) only. Thus, our model does not provide any information of OH(v≤2). Furthermore, it cannot distinguish between OH(5) and OH(4) as well as OH(9) and OH(8), and consequently errors in OH(5) and OH(9) might be compensated by errors in OH(4) and OH(8) or vice versa. Finally, we

our model do not affect the two main conclusions drawn in this study.

Justified by a nearly linear relation between $[O(^3P)]$ and OH(9-7)+OH(8-6) VER, the physically allowed upper limit of $[O(^3P)]$, and also considering the chemical equilibrium of O_3, we conclude that the $[O(^3P)]$ and [H] profiles derived by the Best fit model are plausible in the altitude range from 80 km to 95 km. The corresponding 1σ uncertainty due to uncertainties of chemical reactions and physical processes varies between 35 % and 40 % ([H]) and between 30 % and 40 % ($[O(^3P)]$), depending on altitude.

The [H] derived here is systematically larger by a factor of 1.5 than SABER [H] reported in Mlynczak et al. (2018) which is primarily attributed to their slower OH(ν=8)+O_2 rate. Our $[O(^3P)]$ values in the altitude region below ~87 km are in agreement within the corresponding errors with the results found in Mlynczak et al. (2018) and Zhu and Kaufmann (2018) but are lower than the values presented in Panka et al. (2018). However, we think that the results of the latter study are too large because the authors falsely assumed too fast OH(ν)+O_2 rates. In the altitude region above ~87 km, the $[O(^3P)]$ shown here is generally larger than the values reported in these three studies up to a factor 1.5 to 1.7. These differences are attributed to the faster rates and different deactivation channels of OH(ν)+$O(^3P)$. Therefore, it is indicated that we might overestimate $[O(^3P)]$ above >87km and we suggest that our results should be interpreted as an upper limit. However, a final conclusion cannot be drawn at this point due the large uncertainties of the rates assumed to derive $[O(^3P)]$.

Gelöscht: But these issues will only be solved eventually when future laboratory experiments provide the corresponding OH(ν)+O_2 and OH(ν)+$O(^3P)$ relaxation rates.¶

Gelöscht: chemical equilibrium of O_3 and

Gelöscht: 20

Gelöscht: 30

Data availability

The data used in this study are open for public. The TIMED/SABER data can be downloaded from http://saber.gats-inc.com/data.php while ENVISAT/SCIAMACHY can be accessed by getting in contact with Christian von Savigny (csavigny@physik.uni-greifswald.de).

Author contribution

MS initialized and supervised the study. CVS retrieved the SCIAMACHY data. TF performed the model runs and wrote the final script with contributions from all co-authors.

Competing interests

The authors declare that they have no conflict of interest.

Acknowledgments

T. Fytterer and M. Sinnhuber gratefully acknowledge funding by the Deutsche Forschungsgemeinschaft (DFG), grant SI 1088/6-1. The authors also acknowledge support by the Open Access Publishing Fund of Karlsruhe Institute of Technology.

References

Adler-Golden, S.: Kinetic parameters for OH nightglow modeling consistent with recent laboratory measurements, J. Geophys. Res., 102, 19,969–19,976, doi:10.1029/97JA01622, 1997.

Adrews, D. G., Holton, J. R., and Leovy, C. B. (Eds.): Middle Atmosphere Dynamics, Academic Press, Orlando, USA, 1987.

Anlauf, K. G., MacDonald, R. G., and Polanyi, J. C.: Infrared chemiluminescence from $H+O_3$, at low pressure, Chem. Phys. Lett, 1, 619-622, doi:10.1016/0009-2614(68)80097-1, 1968.

Bovensmann, H., Burrows, J. P., Buchwitz, M., Frerick, J., Noël, S., Rozanov, V. V., Chance, K. V., and Goede, A. P. H.: SCIAMACHY: Mission objectives and measurement modes, J. Atmos. Sci., 56, 127–150, doi:10.1175/1520-0469(1999)056<0127:SMOAMM>2.0.CO;2, 1999.

Bramstedt, K., Noël, S., Bovensmann, H., Gottwald, M., and Burrows, J. P.: Precise pointing knowledge for SCIAMACHY solar occultation measurements, Atmos. Meas. Tech., 5, 2867–2880, doi:10.5194/amt-5-2867-2012, 2012.

Brooke, J. S. A., Bernath, P. F., Western, C. M., Sneden, C., Afsar, M., Li, G., and Gordon, I. E.: Line strengths of rovibrational and rotational transitions in the $X^2\Pi$ ground state of OH, J. Quant. Spectrosc. Ra., 168, 142-157, doi:10.1016/j.jqsrt.2015.07.021, 2016.

Burkholder, J. B., Sander, S. P., Abbatt, J., Barker, J. R., Huie, R. E., Kolb, C. E., Kurylo, M. J., Orkin, V. L., Wilmouth, D. M., and Wine, P. H.: Chemical Kinetics and Photochemical Data for Use in Atmospheric Studies, Evaluation No. 18, JPL Publication 15-10, Jet Propulsion Laboratory, Pasadena,

http://jpldataeval.jpl.nasa.gov, 2015.

Burtt, K. D. and Sharma, R. D.: Near-resonant energy transfer from highly vibrationally excited OH to N_2, J. Chem. Phys., 128, 124311-1 to 124311-8, doi:10.1063/1.2884343, 2008.

Caridade, P. J. S. B., Sabin, J., Garridoz, J. D., and Varandas, A. J. C.: Dynamics of OH + O_2 vibrational relaxation processes, Phys. Chem. Chem. Phys., 4, 4959-4969, doi:10.1039/b203101a, 2002.

Caridade, P. J. S. B., Horta, J. Z. J., and Varandas, A. J. C.: Implications of the O + OH reaction in hydroxyl nightglow modeling, Atmos. Chem. Phys, 13, 1-13, doi:10.5194/acp-13-1-2013, 2013.

Chalamala, B. R. and Copeland, R. A.: Collision dynamics of OH($X^2\Pi$, v=9), J. Chem. Phys., 99, 5807-5811, doi:10.1063/1.465932, 1993.

Charters, P. E., Macdonald, R. G., and Polanyi, J. C.: Formation of vibrationally excited OH by the reaction H+O_3, Appl. Optics, 10, 1747-1754, doi:10.1364/AO.10.001747, 1971.

Dodd, J. A., Lipson, S. J., and Blumberg, W. A. M.: Formation and vibrational relaxation of OH($X^2\Pi_i$,v) by O_2 and CO_2, J. Chem. Phys., 95, 5752-5762, doi:10.1063/1.461597, 1991.

Dyer, M. J., Knutsen, K., and Copeland, R. A.: Energy transfer in the ground state of OH: Measurements of OH(v=8,10,11) removal, J. Chem. Phys., 107, 7809-7815, doi:10.1063/1.475094, 1997.

Finlayson-Pitts, B. J. and Kleindienst, T. E.: The reaction of hydrogen atoms with ozone as a source of vibrationally excited $OH(X^2\Pi_i)_{v=9}$ for kinetic studies, J. Chem. Phys., 74, 5643-5658, doi:10.1063/1.440928, 1981.

García-Comas, M., López-Puertas, M., Marshall, B. T., Wintersteiner, P. P., Funke, B., Bermejo-Pantaleón, D., Mertens, C. J., Remsberg, E. E., Gordley, L. L., Mlynczak, M. G., and Russell III, J. M.: Errors in Sounding of the Atmosphere using Broadband Emission Radiometry (SABER) kinetic temperature caused by non-local-thermodynamic-equilibrium model parameters, J. Geophys. Res., 113, D24106, doi:10.1029/2008JD010105, 2008.

Good, R. E.: Determination of atomic oxygen density from rocket borne measurements of hydroxyl airglow, Planet. Space Sci., 24, 389–395, doi:10.1016/0032-0633(76)90052-0, 1976.

Gottwald, M., Krieg, E., von Savigny, C., Noël, S., Bovensmann, H., and Bramstedt, K.: Determination of SCIAMACHY Line of Sight Misalignments, Proceedings of the Envisat Atmospheric Science

Conference, ESA SP-636, Montreux, Switzerland, 23–27 April, 2007.

Grygalashvyly, M., Sonnemann, G. R., Lübken, F.-J., Hartogh, P., and Berger, U.: Hydroxyl layer: Mean state and trends at midlatitudes, J. Geophys. Res. Atmos., 119, 12,391–12,419, doi:10.1002/2014JD022094, 2014.

Howell, C. D., Michelangeli, D. V., Allen, M., Yung, Y. L., and Thomas, R. J.: SME observations of $O_2(^1\Delta_g)$ nightglow: An assessment of the chemical production mechanisms, Planet. Space Sci., 38, 529-537, doi:10.1016/0032-0633(90)90145-G, 1990.

Kalogerakis, K. S., Smith, G. P., and Copeland, R. A.: Collisional removal of $OH(X^2\Pi, v = 9)$ by O, O_2, O_3, N_2, and CO_2, J. Geophys. Res., 116, D20307, doi:10.1029/2011JD015734, 2011.

Kalogerakis, K. S., Matsiev, D., Sharma, R. D., and Wintersteiner, P. P.: Resolving the mesospheric nighttime 4.3 μm emission puzzle: Laboratory demonstration of new mechanism for OH(υ) relaxation, Geophys. Res. Lett., 43, 8835–8843, doi:10.1002/2016GL069645, 2016.

Kaufmann, M., Lehmann, C., Hoffmann, L., Funke, B., Lopez-Puertas, M., von Savigny, C., and Riese, M.: Chemical heating rates derived from SCIAMACHY vibrationally excited OH limb emission spectra, Adv. Space Res., 41, 1914–1920, doi:10.1016/j.asr.2007.07.045, 2008.

Klenerman, D. and Smith, I. W. M.: Infrared chemiluminescence studies using a SISAM spectrometer, J. Chem. Soc., Farad. T. 2, 83, 229-241, doi:10.1039/F29878300229, 1987.

Knutsen, K., Dyer, M. J., and Copeland, R. A.: Collisional removal of $OH(X^2\Pi)$,v=7) by O_2, N_2, CO_2, and N_2O, J. Chem. Phys., 104, 5798-5802, doi:10.1063/1.471311, 1996.

Kulikov, M. Y., Belikovich, M. V., Grygalashvyly, M., Sonnemann, G. R., Ermakova, T. S., Nechaev, A. A., and Feigin, A. M.: Nighttime ozone chemical equilibrium in the mesopause region. J. Geophys. Res.-Atmos., 123, 1-15, doi:10.1002/2017JD026717, 2018.

Lacoursiere, J., Dyer, M. J., and Copeland, R. A.: Temperature dependence of the collisional energy transfer of OH(ν=10) between 220 and 310 K, J. Chem. Phys., 118, 1661-1667, doi:10.1063/1.1530581, 2003.

López-Puertas, M., García-Comas, M., Funke, B., Picard, R. H., Winick, J. R., Wintersteiner, P. P., Mlynczak, M. G., Mertens, C. J., Russell III, J. M., and Gordley, L. L.: Evidence for an OH(ν) excitation mechanism of CO_2 4.3 μm nighttime emission from SABER/TIMED measurements, J.

Geophys. Res., 109, D09307, doi:10.1029/2003JD004383, 2004.

López-Puertas, M., García-Comas, M., Funke, B., Gardini, A., Stiller, G. P., von Clarmann, T., Glatthor, N., Laeng, A., Kaufmann, M., Sofieva, V. F., Froidevaux, L., Walker, K. A., and Shiotani, M.: MIPAS observations of ozone in the middle atmosphere, Atmos. Meas. Tech., 11, 2187-2212, doi: 10.5194/amt-11-2187-2018, 2018.

Meinel, A. B.: OH Emission Bands in the Spectrum of the Night Sky. II, Astrophys. J., 112, 120-130, doi:10.1086/145321, 1950.

Mlynczak, M. G. and Solomon, S.: A detailed evaluation of the heating efficiency in the middle atmosphere, J. Geophys. Res., 98, 10,517–10,541, doi:10.1029/93JD00315, 1993.

Mlynczak, M. G., Martin-Torres, F. J., Johnson, D. G., Kratz, D. P., Traub, W. A., and Jucks, K.: Observations of the O(^{3}P) fine structure line at 63 mm in the upper mesosphere and lower thermosphere, J. Geophys. Res., 109, A12306, doi:10.1029/2004JA010595, 2004.

Mlynczak, M. G., Martin-Torres, F. J., Crowley, G., Kratz, D. P., Funke, B., Lu, G., Lopez-Puertas, M., Russell III, J. M., Kozyra, J., Mertens, C., Sharma, R., Gordley, L., Picard, R., Winick, J., and Paxton, L.: Energy transport in the thermosphere during the solar storms of April 2002, J. Geophys. Res., 110, A12S25, doi:10.1029/2005JA011141, 2005.

Mlynczak, M. G., Hunt, L. A., Mast, J. C., Marshall, B. T., Russell III, J. M., Smith, A. K., Siskind, D. E., Yee, J.-H., Mertens, C. J., Martin-Torres, F. J., Thompson, R. E., Drob, D. P., and Gordley L. L.: Atomic oxygen in the mesosphere and lower thermosphere derived from SABER: Algorithm theoretical basis and measurement uncertainty, J. Geophys. Res.-Atmos., 118, 5724–5735, doi:10.1002/jgrd.50401, 2013a.

Mlynczak, M. G., Hunt, L. H., Mertens, C. J., Marshall, B. T., Russell III, J. M., López-Puertas, M., Smith, A. K., Siskind, D. E., Mast, J. C., Thompson, R. E., and Gordley, L. L.: Radiative constraints on the global annual mean atomic oxygen concentration in the mesopause region, J. Geophys., Res.-Atmos., 118, 5796-5802, doi:10.1002/jgrd.50400, 2013b.

Mlynczak ,M. G., Hunt, L. A. , Marshall, B. T., Mertens, C. J., Marsh, D. R., Smith, A. K., Russell III, J. M., Siskind, D. E., and Gordley, L. L.: Atomic hydrogen in the mesopause region derived from SABER: Algorithm theoretical basis, measurement uncertainty, and results, J. Geophys. Res.-Atmos., 119, 3516–

3526, doi:10.1002/2013JD021263, 2014.

Mlynczak, M. G., Hunt, L. A., Russell III, J. M., and Marshall, B. T.: Updated SABER Night Atomic Oxygen and Implications for SABER Ozone and Atomic Hydrogen, Geophys. Res. Lett., 45, 5735-5741, doi:10.1029/2018GL077377, 2018.

Murtagh, D. P., Witt, G., Stegman, J., McDade, J. C., Llewellyn, E. J., Harris, F., and Greer, R. G. H.: An assessment of proposed O(^{1}S) and $O_2(b^1\Sigma_g^+)$ nightglow excitation parameters, Planet. Space Sci., 38, 43-53, doi:10.1016/0032-0633(90)90004-A, 1990.

Nelson Jr., D. D., Schiffman, A., Nesbitt, D. J., Orlando, J. J., and Burkholder, J. B.: H + O_3 Fourier-transform infrared emission and laser absorption sudies of OH($X^2\Pi$) radical: An experimental dipole moment function and state-to-state Einstein A coefficients, J. Chem. Phys., 93, 7003-7019, doi:10.1063/1.459476, 1990.

Ohoyama, H., Kasai, T., Yoshimura, Y., Kimura, H., and Kuwata, K.: Initial distribution of vibration of the OH radicals produced in the H+O_3 → OH($X^2\Pi_{1/2,3/2}$)+O_2 reaction: Chemiluminescence by a crossed beam technique, Chem. Phys. Lett., 118, 263-266, doi:10.1016/0009-2614(85)85312-4, 1985.

Panka, P. A., Kutepov, A. A., Kalogerakis, K. S., Janches, D., Russell III, J. M., Rezac, L., Feofilov, A. G., Mlynczak, M. G., and Yigit, E.: Resolving the mesospheric nighttime 4.3 μm emission puzzle: comparing the CO2(ν_3) and OH(ν) emission models, Atmos. Chem. Phys., 17, 9751-9760, doi:10.5194/acp-17-9751-2017, 2017.

Panka, P. A., Kutepov, A. A., Rezac, L., Kalogerakis, K. S., Feolilov, A. G., Marsh, D., Janches, D., and Yigit, E.: Atomic Oxygen Retrieved From the SABER 2.0- and 1.6-μm Radiances Using New First-Principles Nighttime OH(v) Model, Geophys. Res. Lett., 45, 5798-5803, doi:10.1029/2018GL077677, 2018.

Rensberger, K. J., Jeffries, J. B., and Crosley, D. R.: Vibrational relaxation of OH($X^2\Pi_i$,v=2), J. Chem. Phys., 90, 2174-2181, doi:10.1063/1.456671, 1989.

Rothman, L. S., Gordon, I .E., Barbe, A., Benner, D. C., Bernath, P. F., Birk, M., Boudon, V., Brown, L. R., Campargue, A, Champion, J.-P., Chance, K., Coudert, L. H., Danaj, V., Devi, V. M., Fally, S., Flaud, J.-M., Gamache, R. R., Goldmanm, A., Jacquemart, D., Kleiner, I., Lacome, N., Lafferty, W. J., Mandin, J.-Y., Massie, S. T., Mikhailenko, S. N., Miller, C. E., Moazzen-Ahmadi, N., Naumenko, O. V., Nikitin,

A. V., Orphal, J., Perevalov, V. I., Perrin, A., Predoi-Cross, A., Rinsland, C. P., Rotger, M., Simeckova, M., Smith, M. A. H., Sung, K., Tashkun, S. A., Tennyson, J., Toth, R. A., Vandaele, A. C., Vander Auwera, J.: The HITRAN 2008 molecular spectroscopic database, J. Quant. Spectrosc. Ra., 110, 533–572, doi:10.1016/j.jqsrt.2009.02.013, 2009.

Russell, J. P. and Lowe, R. P.: Atomic oxygen profiles (80–94 km) derived from Wind Imaging Interferometer/Upper Atmospheric Research Satellite measurements of the hydroxyl airglow: 1. Validation of technique, J. Geophys. Res., 108, 4662, doi:10.1029/2003JD003454, 2003.

Russell, J. P., Ward, W. E., Lowe, R. P., Roble, R. G., Shepherd, G. G., and Solheim, B.: Atomic oxygen profiles (80 to 115 km) derived from Wind Imaging Interferometer/Upper Atmospheric Research Satellite measurements of the hydroxyl and greenline airglow: Local time–latitude dependence, J. Geophys. Res., 110, D15305, doi:10.1029/2004JD005570, 2005.

Russell III, J. M., Mlynczak, M. G., Gordley, L. L., Tansock, J., and Esplin, R.: An overview of the SABER experiment and preliminary calibration results, in Proceedings of the 44th Annual Meeting, Denver, Colorado, July 18–23, vol. 3756, pp. 277–288, SPIE, Bellingham, WA, 1999.

Sander, R., Baumgaertner, A., Gromov, S., Harder, H., Jöckel, P., Kerkweg, A., Kubistin, D., Regelin, E., Riede, H., Sandu, A., Taraborrelli, D., Tost, H., and Xie, Z.-Q.: The atmospheric chemistry model CAABA/MECCA-3.0, Geosci. Model Dev., 4, 373-380, doi:10.5194/gmd-4-373-2011, 2011.

Shalashilin, D. V., Umanskii, S. Y., and Gershenzon, Y. M.: Dynamics of vibrational energy exchange in collisions of OH and OD radicals with N_2. Application to the kinetics of OH-vibrational deactivation in the upper atmosphere, Chem. Phys., 168, 315-325, doi:10.1016/0301-0104(92)87165-6, 1992.

Shalashilin, D. V., Michtchenko, A. V., Umanskii, S. Y., and Gershenzon, Y. M.: Simulation of Effective Vibrational-Translational Energy Exchange in Collisions of Vibrationally Excited OH with O_2 on the Model Potential Energy Surface. Can the Relaxation of OH(ν) Be One-Quantum for Low and Multiquantum for High v?, J. Phys., Chem.-US, 99, 11627-11635, doi:10.1021/j100030a001, 1995.

Sharma, R. D., Wintersteiner, P. P., and Kalogerakis, K. S.: A new mechanism for OH vibrational relaxation leading to enhanced CO_2 emissions in the nocturnal mesosphere, Geophys. Res. Lett., 42, 4639–4647, doi:10.1002/2015GL063724, 2015.

Sharp, W. E. and Kita, D.: In situ measurement of atomic hydrogen in the upper mesosphere, J.

Geophys. Res.-Atmos., 92, 4319–4324, doi:10.1029/JD092iD04p04319, 1987.

Smith, A. K., Marsh, D. R., Mlynczak, M. G., and Mast, J. C.: Temporal variation of atomic oxygen in the upper mesosphere from SABER, J. Geophys. Res., 115, D18309, doi:10.1029/2009JD013434, 2010.

Smith, A. K., Harvey, V. L., Mlynczak, M. G., Funke, B., García-Comas, M., Hervig, M., Kaufmann, M., Kyrölä, E., López-Puertas, M., McDade, I., Randall, C. E., Rusell III, J. M., Sheese, P. E., Shiotani, M., Skinner, W. R., Suzuki, M., and Walker, K. A.: Satellite observations of ozone in the upper mesosphere, J. Geophys. Res.-Atmos., 118, 5803-5821, doi:10.1002/jgrd.50445, 2013.

Streit, G. E. and Johnston, H. S.: Reactions and quenching of vibrationally excited hydroxyl radicals, J. Chem. Phys., 64, 95-103, doi:10.1063/1.431917, 1976.

Thiebaud, J. E., Copeland, R. A, and Kalogerakis, K. S.: Vibrational relaxation of OH(v=7) with O, O_2 and H, Abstract SA43A-1752, Fall Meeting, AGU, San Francisco, Calif, 2010.

Turnbull, D. N. and Lowe, R. P.: New hydroxyl transition probabilities and their importance in airglow studies, Planet. Space Sci., 37, 723–738, doi:10.1016/0032-0633(89)90042-1, 1989.

Van der Loo, M. P. J., and Groenenboom, G. C.: Theoretical transition probabilities for the OH Meinel system, J. Chem. Phys., 126, 114413, doi: 10.1063/1.2646859, 2007.

Varandas, A. J. C.: Reactive and non-reactive vibrational quenching in O + OH collisions, Chem. Phys. Lett., 396, 182-190, doi:10.1016/j.cplett.2004.08.023, 2004.

Von Savigny, C. and Lednyts'kyy, O.: On the relationship between atomic oxygen and vertical shifts between OH Meinel bands originating from different vibrational levels, Geophys. Res. Lett., 40, 5821-5825, doi:10.1002/2013GL058017, 2013.

Von Savigny, C., McDade, I. C., Eichmann, K.-U., and Burrows, J. P.: On the dependence of the OH* Meinel emission altitude on vibrational level: SCIAMACHY observations and model results, Atmos. Chem. Phys., 12, 8813–8828, doi:10.5194/acp-12-8813-2012 , 2012.

Xu, J., Gao, H., Smith, A. K., and Zhu, Y.: Using TIMED/SABER nightglow observations to investigate hydroxyl emission mechanisms in the mesopause region, J. Geophys. Res., 117, D02301, doi:10.1029/2011JD016342, 2012.

Zhu, Y., and Kaufmann, M.: Atomic oxygen abundance retrieved from SCIAMACHY hydroxyl nightglow measurements, Geophys. Res. Lett., 45, 1-9, doi:10.1029/2018GL079259, 2018.

Table 1. Physical processes and chemical reactions included in the Base model

	Process	Rate or scheme	Reference
R1	$H + O_3 \rightarrow OH(\nu) + O_2$	$k_1 = 1.4\times10^{-10}\ e^{(-470/T)}$ $k_1(\nu) = k_1\ f_1(\nu)$[a]	Burkholder et al. (2015), Alder-Golden (1997, Table 1)
R2	$O(^3P) + O_3 \rightarrow O_2 + O_2$	$k_2 = 8\times10^{-12}\ e^{(-2060/T)}$	Burkholder et al. (2015)
R3	$O(^3P) + O_2 + M \rightarrow O_3 + M$	$k_3 = 6\times10^{-34}\ (300/T)^{2.4}$	Burkholder et al. (2015)
R4	$OH(\nu) \rightarrow OH(\nu') + h\nu$	variable rates	Xu et al. (2012, Table A1)
R5	$OH(\nu) + N_2 \rightarrow OH(\nu') + N_2$	$\nu'=\nu-1$	Adler-Golden (1997, Table 1), Kalogerakis et al. (2011)
R6	$OH(\nu) + O_2 \rightarrow OH(\nu') + O_2$	$\nu'<\nu$	Adler-Golden (1997, Table 3), see text for more information
R7a	$OH(\nu) + O(^3P) \rightarrow H + O_2$	variable rates	Varandas (2004, Table 3, M I)
R7b	$OH(\nu) + O(^3P) \rightarrow OH(\nu') + O(^3P)$	$\nu'<\nu$	Caridade et al. (2013, Table 1)

Rate constants are given in the cm^3-s^{-1} system.

[a] $f_1(5, 6, 7, 8, 9) = 0.01, 0.03, 0.15, 0.34, 0.47$

Table 2. Empirically determined branching ratios of $OH(\nu)+O_2 \rightarrow OH(\nu')+O_2$ of the O_2 best fit model based on OH(6-2) VER, OH(5-3)+OH(4-2) VER, and OH(3-1) VER observations.

Gelöscht: below 85 km

ν/ν'	**8**	**7**	**6**	**5**	**4**	**3**	**≤2**
9	0	0	0	0	1	0	0
8		0	0	0	0.3	0.7	0
7			0	0	0	0.1	0.9
6				0	0	0	1
5					0	0	1
4						0	1
3							1

Table 3. Empirically determined branching ratios of $OH(v)+O(^3P)\rightarrow OH(v')+O(^1D)$ of the Best fit model based on OH(6-2) VER, OH(5-3)+OH(4-2) VER, and OH(3-1) VER observations.

	Process	Recommendation	Best fit rate ($cm^3\ s^{-1}$)
R11a	$OH(9) + O(^3P) \rightarrow OH(4) + O(^1D)$	$k_{11}(9\text{-}4) > 0.6\times k_{11}(v=9)$	$0.8\times2.30\times10^{-10}$
R11b	$OH(9) + O(^3P) \rightarrow OH(3) + O(^1D)$	not negligible	$0.2\times2.30\times10^{-10}$
R11c	$OH(8) + O(^3P) \rightarrow OH(3) + O(^1D)$	$k_{11}(v=8) < k_{11}(v=9)$	$1.0\times1.80\times10^{-10}$
R11d	$OH(7) + O(^3P) \rightarrow OH(\leq2) + O(^1D)$	$k_{11}(7\text{-}\leq2) < k_{11}(v=8)$	1.25×10^{-10}
R11fe	$OH(6) + O(^3P) \rightarrow OH(\leq1) + O(^1D)$	$k_{11}(6\text{-}\leq1) < k_{11}(v=7)$	0.80×10^{-10}
R11gf	$OH(5) + O(^3P) \rightarrow OH + O(^1D)$	$k_{11}(v=5) < k_{11}(v=6)$	0.40×10^{-10}

Gelöscht: above 85 km

Gelöscht: 9

Gelöscht: $0.2\times2.30\times10^{-10}$

Gelöscht: 9

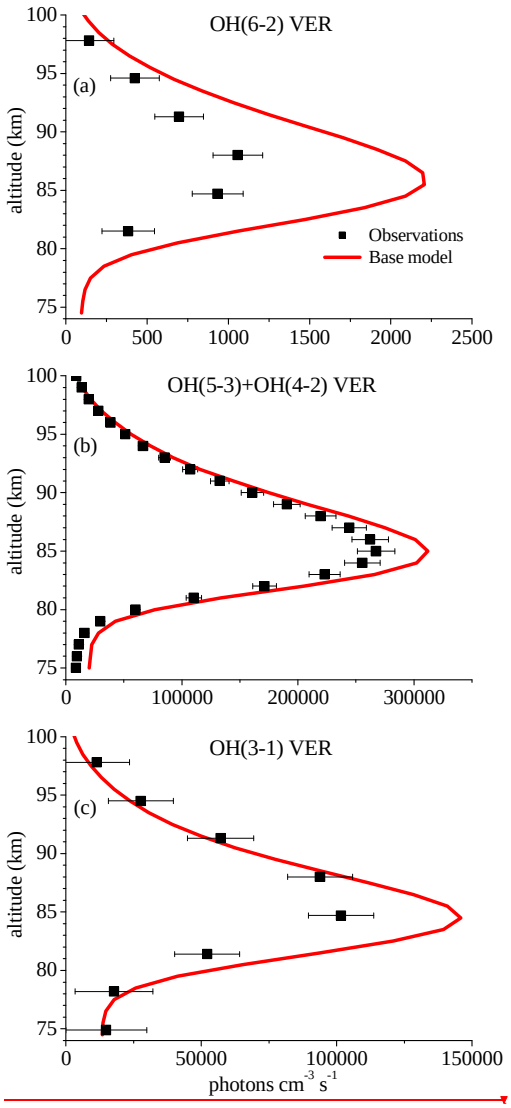

Gelöscht:

925 **Figure 1 : Comparison of vertical profiles of the volume emission rate (VER) of a) OH(6-2), b) OH(5-3)+OH(4-2), and c) OH(3-1) at 0°-10° N between satellite observations and the Base model output. The observations are climatology of night-time mean zonal means from 2003 to 2011, based on co-location measurements of TIMED/SABER and ENVISAT/SCIAMACHY. Note the different scaling of the x-axis.**

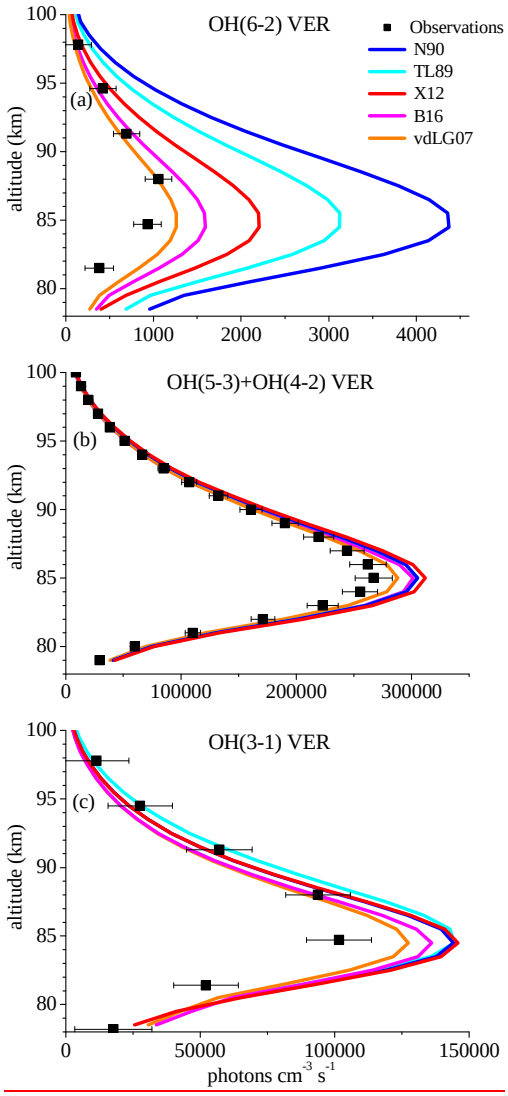

930 **Figure 2 :** Same as Figure 1 but for different sets of Einstein coefficients from literature, namely N90 (Nelson et al., 1990), TL89 (Turnbull and Lowe, 1989), X12 (=Base model; Xu et al., 2012), B16 (Brooke et al., 2016), and vdLG07 (van der Loo and Groenenboom, 2007).

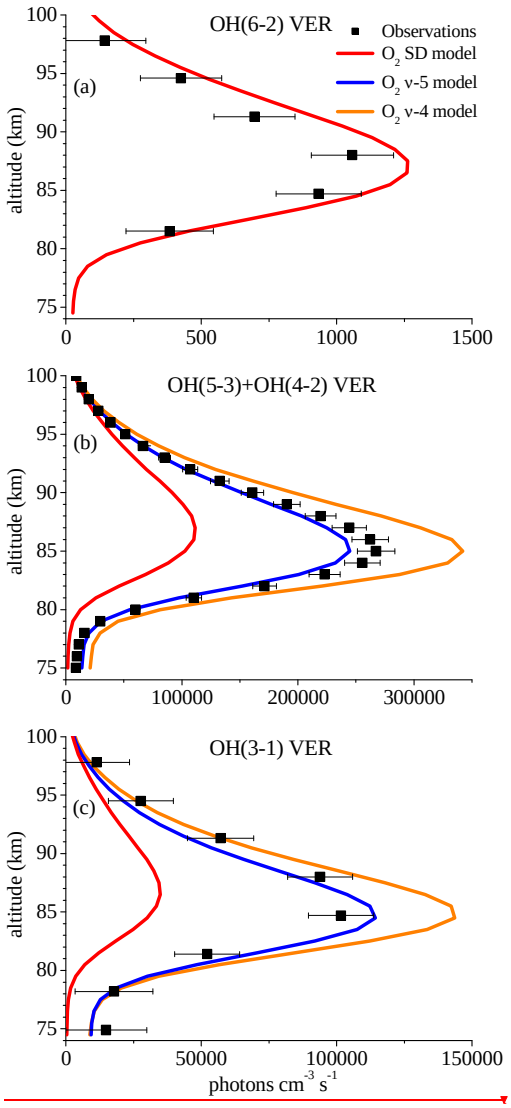

Figure 3: Same as Fig. 1 but for the O_2 SD model, the O_2 ν-5 model, and the O_2 ν-4 model. Note that the results of these three models are identical in case of OH(6-2) VER.

Gelöscht:

Gelöscht: 2

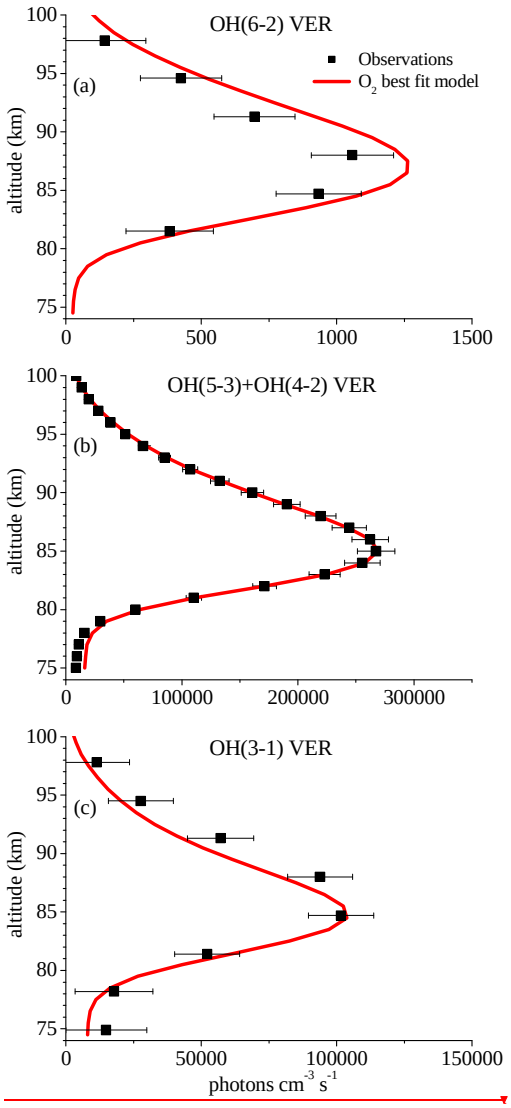

Figure 4: Same as Fig. 1 but for the O_2 best fit model. Note that Fig. 4a is identical to Fig. 3a but was plotted again for convenience.

Gelöscht:

Gelöscht: 3

Gelöscht: 3

Gelöscht: 2

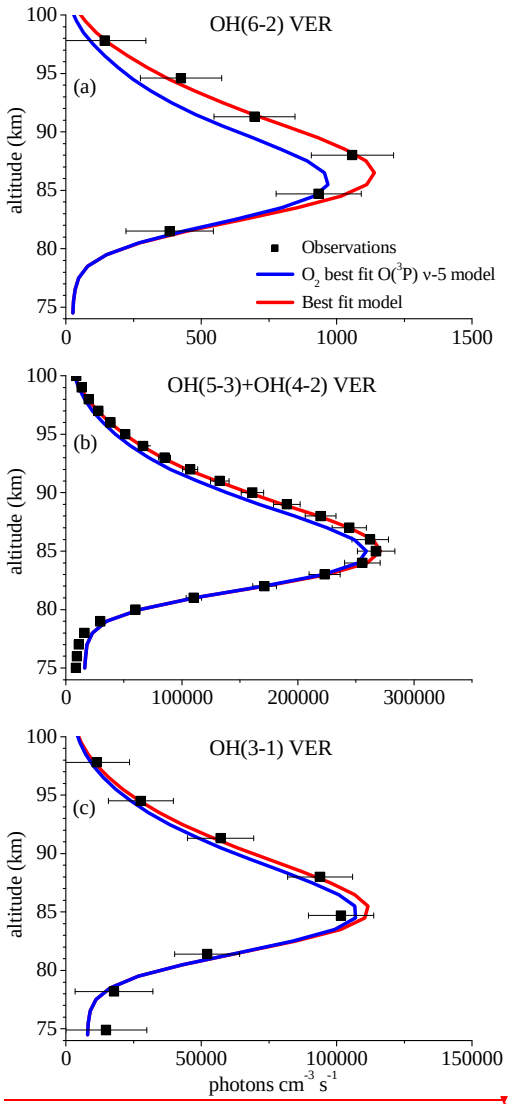

Figure 5: Same as Fig. 1 but for the O_2 best fit $O(^3P)$ v-5 model and the Best fit model.

Gelöscht:

Gelöscht: 4

945

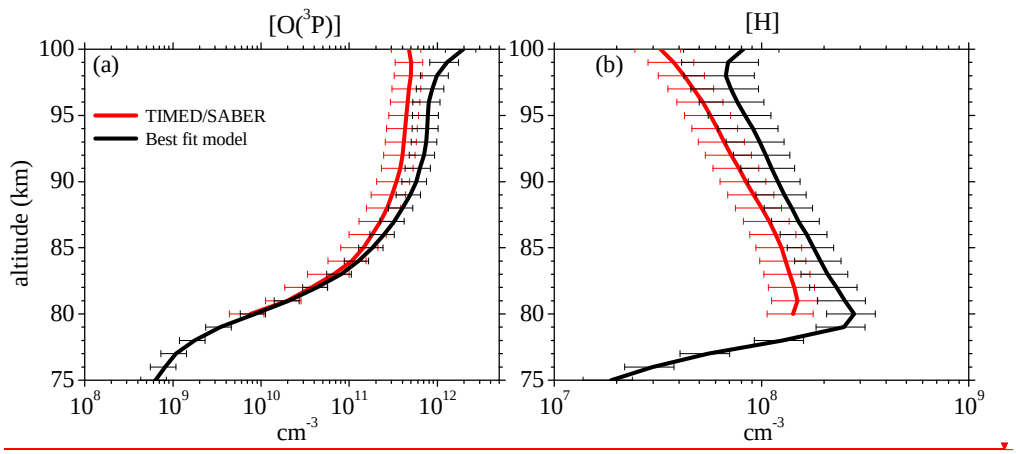

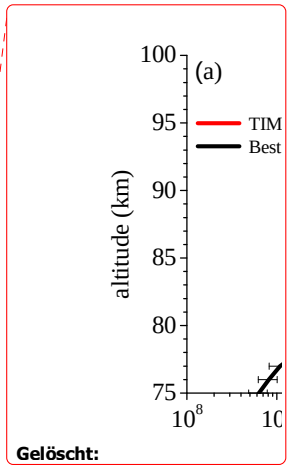

Gelöscht:

Gelöscht: 5

Figure 6 : Vertical profiles of a) O(3P) and b) [H] derived from SABER OH(9-7)+OH(8-6) VER observations (Mlynczak et al., 2018) and our Best fit model by fitting SABER OH(9-7)+OH(8-6) VER and OH(5-3)+OH(4-2) VER as well as SCIAMACHY OH(6-2) VER and OH(3-1) VER. Shown are averages of night-time mean zonal means of co-location measurements (see Sect. 2.2) from 2003 to 2011 between 0° and 10° N. Error bars show the 1σ uncertainty due to chemical and physical processes.

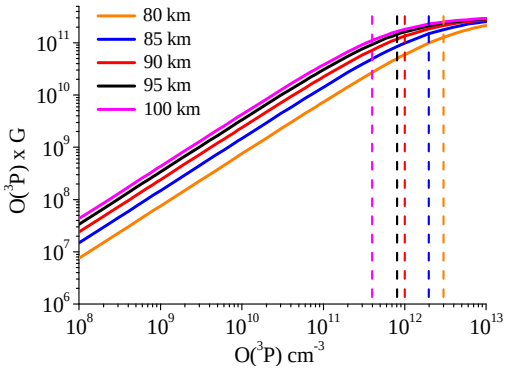

Figure 7: $O(^3P)\times G$ as a function of $O(^3P)$ at different altitudes. The visually determined upper limits of $O(^3P)$ before non-linearity becomes too pronounced are represented by the dashed lines.

Gelöscht: 6